Green Chemistry

TUTORIAL REVIEW

View Article Online
View Journal | View Issue

Cite this: *Green Chem.*, 2024, **26**, 9048

The advanced applications of ionic liquids in new energy, electronic information materials, and biotechnologies

Suojiang Zhang, *[a,b] Yuhong Huang, [a] Lan Zhang,[a] Yanrong Liu, [a] Qingqing Miao,[a] Ruixia Liu, [a] Weizhen Zhao, [a] Yanyan Diao [a] and Kun Dong[a]

Received 28th March 2024,
Accepted 9th July 2024

DOI: 10.1039/d4gc01519c

rsc.li/greenchem

Ionic liquids (ILs) with remarkable performance offer opportunities to advance green and low-carbon chemical processes. Thus, much work is focused on building an innovative theory and knowledge framework to unravel the nature of ILs. Moreover, there is an increasing trend to utilize ILs in rapidly emerging fields. Aiming to provide an overview of the recent advances and challenges of ILs in the development of green processes for renewable resources, this review highlights the properties and functions of ILs in IL gating and as electrolyte additives, modifiers, exfoliation agents, nucleation substrates, tunable solvents, versatile carriers and biosensor components in three representative and revolutionary production processes, namely, new energy, electronic information materials, and biotechnologies. The innovative applications of ILs demonstrate their potential to create a landscape of low-carbon, high-end and smart technologies.

Introduction

Ionic liquids (ILs) have emerged as a fascinating and versatile class of functional solvents/materials with a wide range of applications,[1,2] and their utilization in the emerging fields of new energy (various forms of energy other than traditional energy sources such as coal, petroleum, and natural gas), electronic materials, and biotechnologies have attracted significant attention in recent years.[3] Their environmentally friendly nature and tunable physicochemical properties, such as melting point, viscosity, and polarity, make them well-suited for the development of green and low-carbon chemical processes.

The investigation of ILs comprise four historical phases. First-generation ILs can be dated back to 1914 when Walden first synthesized ethylammonium nitrate [$EtNH_3$][NO_3] with a melting point of 12 °C.[4] Subsequently, Hurley and Wier pioneered the application of ILs by adding ethylpyridinium bromide to aluminum chloride to synthesize the colorless and transparent IL chloroaluminate during heating.[5] Thereafter, the design and synthesis of room-temperature molten salts together with their electrochemical applications became the focus of research on first-generation ILs. It was not until 1992 that IL research progressed to second-generation ILs with the first report on air- and water-stable 1-ethyl-3-methylimidazolium based ILs 1-ethyl-3-methylimidazolium tetrafluoroborate ([EtMeim][BF_4]) and 1-ethyl-3-methylimidazolium acetate ([EtMeim][$MeCO_2$]).[6] After 2000, with the research emphasis shifting from the stability of ILs to their structural designability, functionalized ILs or designer solvents developed rapidly into the third generation in accordance with specific physiochemical needs. Diverse grafted functional groups allowed for the rational design of ILs for various applications in terms of acidity, alkalinity, miscibility, conductivity, chirality, *etc*. In particular, biodegradable and biocompatible third-generation ILs based on choline, amino acids, and carboxylic acids have been developing quickly in green chemical applications. Meanwhile, the relationship of ion-pairs (for example, large sizes and asymmetric shapes) and hydrogen bonding with the properties and roles of ILs in applications has been revealed to support the development of third-generation IL-based applications.[7] Many ILs inherently present bioactivity and have been used in biomedicine in recent years, and this combination is set to open new avenues for discoveries and applications in biochemistry, biomedicine and pharmacology, food science, and nanotechnology.[8] Meanwhile, some theoretical investigations have been carried out to direct the rational design of ILs in biomedical applications. Theoretical approaches allow for the identification of

[a]*Beijing Key Laboratory of Ionic Liquids Clean Process, CAS Key Laboratory of Green Process and Engineering, State Key Laboratory of Mesoscience and Engineering, Institute of Process Engineering, Chinese Academy of Sciences, Beijing 100190, P. R. China. E-mail: sjzhang@ipe.ac.cn*
[b]*Longzihu New Energy Laboratory, Zhengzhou Institute of Emerging Industrial Technology, Henan University, Zhengzhou 450000, P. R. China*

the most likely radical scavenging mechanisms and the corresponding ionic forms under the studied experimental conditions and rationalization of the observed activity differences between salts and acids.[7–9]

More recently, MacFarlane and coworkers[10] proposed fourth-generation ILs based on the exciting combination of the properties of certain mixtures, such as an equal molar mixture of lithium salt and diethylene glycol. This facilitates the evolution of ILs into a broader field of fundamental phenomena and applications. In addition, substantial progress has been made in the multiscale nature and functionality of ILs ranging from Z-bonds to quasi-liquids and ionic clusters.[11,12] Specifically, Z-bonds are formed by hydrogen bonding in ILs coupled with strong electrostatic interactions between their cations and anions, resulting in the formation of aggregates, interfacial ILs/quasi-liquids, and ionic clusters. These complex structures establish various ionic microenvironments and endow ILs with different functionalities compared to ion-pairs. Thus, due to this controlled performance, ILs have been widely applied in many processes, especially in many cutting-edge fields.

As an emerging research area, there is a gap between ILs and advanced materials/technologies (new energy, electronic information materials, and biotechnologies). Thus, herein, we aim to address this gap by presenting an extensive and up-to-date review focusing on the applications of functional ILs in these areas. It is timely and necessary to summarize these achievements for depicting the colourful future of ILs in these emerging research fields. Given that many of these novel applications and modifications are associated with inherent features, we expect that with new properties being continually discovered, scientists in different fields will inspire each other, thus enabling faster and further progress in more sustainable carbon-neutral research. In this review, to highlight the advances in understanding the structure–function–application relationship of ILs, we present several applications of ILs in typical emerging fields, including renewable energy storage and generation (battery, hydrogen energy, and solar cells), electronic information chemicals (two-dimensional materials and photoresists), and biotechnologies (biocatalysis and biomedicine). Although many high-quality reviews in the relevant fields have been published in the past 3 years,[13–18] by providing a tutorial analysis of the recent research and challenges in these areas, we aim to inspire new ideas and avenues for the design of innovative IL and the relevant applications.

IL-driven new energy revolution

ILs and lithium batteries

ILs are promising candidates for electrolyte applications due to their ion-conductive nature, non-flammability, reasonable dielectric constant to dissociate salts, and wide liquid temperature range.[1,19–21] Meantime, their rich anions may potentially contribute to the formation of an inorganic-rich solid electrolyte interphase (SEI) on the anode, thus enhancing the stability of batteries especially those composed of metal anodes.[22,23] Currently, ILs are widely studied as electrolytes for lithium,[24,25] sodium,[26,27] potassium[28] and magnesium batteries.[29] Specifically, a metal-free and solvent-free concept was demonstrated by Qin *et al.*[30] in an all-organic polyimide/1-ethyl-3-methylimidazolium bis(trifluoromethylsulfonyl) imide (EmimTFSI)/polytriphenylamine full-cell. Due to the highly conductive and non-solvation characters of the pure IL electrolyte, the cell showed an outstanding rate capability (up to 200 °C) and wide temperature adaptability, making it a promising candidate for the future energy storage devices. Given that other batteries rely on the reversible insertion/conversion of metal ions (such as Li, Na, K, and Mg), ILs mainly function as ion transport media and participate in the formation of SEI (on both the cathode and anode). Considering the multiple high-quality reviews published recently, which included the major progress on the application of IL in both supercapacitors and major secondary metal (ion) batteries,[13–18] here we employ the lithium battery as an example to illustrate some special functions of ILs, and thus provide some guidelines for future research.

Thus far, ILs have been rarely used in commercialized lithium-ion batteries (LIBs) for the following reasons: (1) the high viscosity of ILs usually slows down the diffusion of Li^+ and influences the battery kinetics; (2) some cations may insert into the graphite layers with Li^+, leading to their exfoliation; and (3) the introduction of ILs also increases the population of both cations and anions, which may reduce the lithium ion transference number (t_{Li^+}) of the electrolyte and hinder the stable plating of lithium.[31] Although these challenges can be partly addressed *via* strategies such as introducing a co-solvent,[22,32] film forming additives,[33] or cation immobilization,[34–37] they largely compromise the benefits of ILs. In this case, the development of high specific capacity non-carbon anodes such as silicon[38–40] and metal lithium[22,37,41] bring about new opportunities for ILs. However, these anodes usually suffer from large volume variation on lithiation, which increases the requirements of the flexibility and stability of SEI beyond the capability of common carbonate electrolytes. Svensson tested the performance of four types of IL electrolytes (lithium bis(fluorosulfonyl)imide (LiFSI) in *N*-methyl-*N*-propylpyrrolidinium bis(fluorosulfonyl)imide ($PYR_{13}FSI$), *N*-methyl-*N*-propylpyrrolidinium bis(trifluoromethylsulfonyl)imide ($PYR_{13}TFSI$), and EmimFSI or trimethyl (isobutyl)phosphonium bis(fluorosulfonyl)imide, $P_{111i4}FSI$) in $LiFePO_4$‖Si pseudo-full cells (in which the cathode area capacity was about 3.54 mA h cm^{-2}, higher than that of 2.68 mA h cm^{-2} of the anode to supply enough active Li) and compared with that of carbonate electrolyte (STD-2).[39] They found that all the IL electrolytes demonstrated better cycle stability than STD-2 except for $PYR_{13}TFSI$ due to its low ionic conductivity and limiting exchange current density (j_0). Also, the cell with the $P_{111i4}FSI$ electrolyte showed the highest average coulombic efficiency (CE) and capacity retention within 100 cycles. However, they also noted that rate capability of the cells with IL electrolytes still need to be enhanced.

Sanchez-Ramirez's group compared the performances of several phosphonium and pyrrolidinium IL electrolytes towards a silicon/poly(acrylonitrile) (Si/PAN) electrode. Similar to Svensson's conclusion, they found the anion has vital influence on the cell performance, where FSI showed much better cycle stability than TFSI, which can be attributed to its inorganic rich SEI. Besides, a reasonable chain length is also an important factor affecting the ion diffusion within the electrolyte.

The application of metal lithium anode is the ultimate goal in battery development, which can not only enable the application of conversion-type cathodes such as sulfur[42] and oxygen,[43] but also compensate for the active lithium loss of insertion-type materials.[44] However, the extremely low standard potential of lithium (−3.014 V *vs.* standard hydrogen electrode) makes it reactive towards most organic solvents, and thus a thin, flexible and ion conductive SEI is vital for its stable long-term operation. Passerini's group studied the lithium nucleation and plating/stripping behaviors in *N*-butyl-*N*-propylpyrrolidinium bis(fluorosulfonyl)imide ($PYR_{14}FSI$)/LiTFSI electrolytes using Ni foil as the current collector *via in situ* atomic force microscopy (AFM) and *ex situ* X-ray photoelectron spectroscopy (XPS).[45] They found that both anions (FSI and TFSI) were reduced with the nucleation of Li, especially the one with a low salt (LiTFSI) content, which is possibly due to the poor Li^+ diffusion. Although the introduction of fluoroethylene carbonate (FEC, 5 wt%) had little influence on the electrolyte viscosity or ionic conductivity, it increased the j_0 and terminated the massive reduction of anions, thus enabling uniform Li nucleation and stable plating/stripping processes. However, the Li||Li symmetric cells could only cycle for about 100 h even at a low current density of 0.08 mA cm^{-2}, and therefore the j_0 of the IL electrolytes still needs to be enhanced to fulfill the requirements of lithium metal batteries (LMBs), in which additional co-solvents are necessary. The same group prepared a localized high concentration electrolyte (LCE) with LiFSI, EmimFSI and monofluorobenzene (mFBn) (1 : 2 : 2 molar ratio).[32] Similar to the case in other LCEs, mFBn reduced the viscosity and increased the conductivity of the electrolyte, and also increased the Li^+ self-diffusion coefficient by 2.5 times. Consequently, the lithium plating stability was greatly enhanced (Fig. 1a) and the Li||Li symmetric cell demonstrated a long cycle life of more than 1500 h under the conditions of 1 mA cm^{-2}/1 mA h cm^{-2}. The authors also believed that mFBn led to the further reduction of FSI, and thus the formation of an inorganic-rich SEI and highly reversible lithium stripping/platting processes. Bao and Cui's group developed a solvent-anchored non-flammable electrolyte (SAFE) by tethering a pyrrolidinium IL on the flexible siloxane chain (PyFSI, Fig. 1b) and dissolved it in a mixture of LiFSI and dimethoxyethane (DME).[37] The optimized SAFE (Fig. 1c) showed a high t_{Li^+} of 0.7, which was attributed to the IL cation anchor effect of siloxane and the interactions among DME, IL and LiFSI, under which a certain ratio of FSI anions entered the solvation structure of Li^+. Consequently, the satisfactory ionic conductivity of 1.6 mS cm^{-1} at room temperature

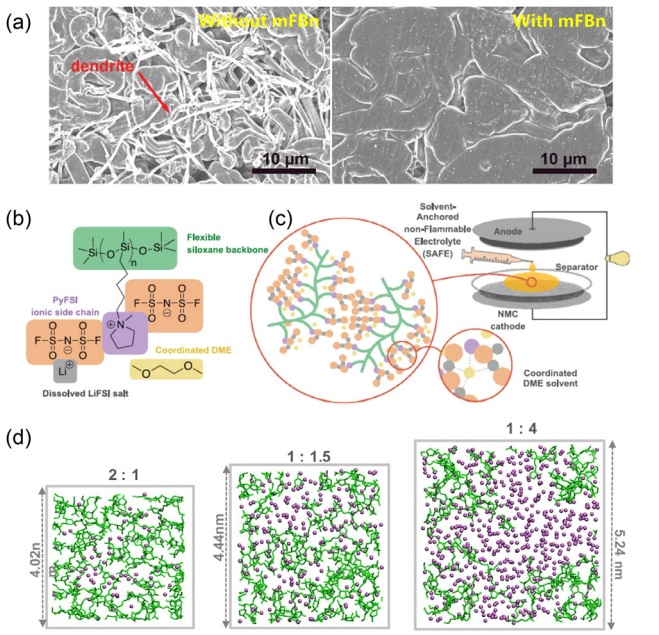

Fig. 1 Advanced IL electrolyte design and its functions in LMBs. (a) SEM pictures of the lithium metal deposition (1.5 mA h cm^{-2}) in IL electrolyte w/o mFBn on Cu foil.[32] (b) Schematic illustration of LiFSI : PyFSI : DME = 1 : 1 : 1 and (c) a schematic of the addition of SAFE to a battery separator and zoomed-in (drawn with the molar ratio of LiFSI : PyFSI : DME = 2 : 1 : 1.5) structure of the complex.[37] Reproduced from ref. 37 with permission from Elsevier, copyright 2023. (d) Snapshots of the simulation box of the PIL-in-salt electrolytes, where the 2 : 1, 1 : 1.5 and 1 : 4 (PIL : salt, molar ratio) systems are listed. It can be noted that with an increase in the salt ratio, more Li^+ ions (purple balls) are present in the polymer matrix (green sticks).[46] Reproduced from ref. 46 with permission from Elsevier, copyright 2019.

and outstanding thermal stability, which could support the cell working in the temperature range of 25–100 °C, were achieved. Besides, the cycle life of the Li||Li cell was more than 600 h at a high current density of 2 mA cm^{-2}.

The use of polymerized ILs (PILs) is another strategy to localize the cation, and thus reduce its influence on t_{Li^+} for the preparation of solid-state lithium metal batteries (SSLMBs). Forsyth's group prepared a poly(diallyldimethylammonium) bis(fluorosulfonyl)imide in-salt (LiFSI) electrolyte.[46] With a molar ratio of 1 : 1.5, the electrolyte showed a satisfactory t_{Li^+} of 0.56 and better electrochemical stability than that of polyethylene oxide (PEO)-based solid polymer electrolytes (SPEs),[47,48] and thus could support the operation of the $Li_{1/3}Ni_{1/3}Mn_{1/3}CoO_2$ SSLMB. PIL could also be used as an interlayer to enhance the compatibility between the electrolyte and anode (Fig. 1d). Based on PyFSI, Bao and Cui[36] further reported the preparation of a salt-philic, solvent-phobic (SP^2) polymer with an IL (pyrrolidinium bis(trifluoromethylsulfonyl) imide (PyTFSI) to interact with the lithium salt) possessing alkyl (to reduce the electrode/electrolyte interfacial energy) and perfluorinated (to repel the organic solvents) functional groups tethered on its siloxane main chain. The SP^2 polymer showed good chemical stability, high selective transport (salt

with priority), and easy coverage properties, on which an anion-derived inorganic-rich robust and stable SEI could be generated. Consequently, the cells with the polymer-coated 50 μm-thick Li anode and 2.5 mA h cm^{-2} lithium nickel manganese cobalt oxide (NMC) cathode demonstrated 400 stable cycles with 80% capacity retention.

In summary, ILs show certain drawbacks in LIB applications due to their incompatibility with graphite, while with the development of Si anodes and LMB, a high-quality SEI is required. Accordingly, due to their intrinsic conductivity, safety, and rich anions, ILs may provide new solutions in these systems. However, currently, the knowledge on IL-based electrolytes is still inadequate to support the rational design of novel battery systems, and thus future studies should pay more attention to the following aspects. Firstly, the interactions between the anion and other solvents should be clarified. The commonly used anions, such as FSI^- and $TFSI^-$ are rich in F, may lead to strong dipole–dipole or H bond interactions with the carbonate, ester, or ether solvents and alter the solvation structure of the anion, thus further influencing the SEI components. Secondly, the rational design of the cation. IL cation immobilization is necessary to increase the metal ion transference number, which will delay or even suppress the formation of dendrites, indicating that one of the roles played by the IL cation is to maintain charge neutrality. The functional groups, such as vinyl, imine, and carboxyl, in ILs can also interact with the cathode and the solvent, participate in the formation of SEI, and thus affect the battery performance. Finally, an in-depth understanding of the interactions between the cation and anion and the dissociation and cluster behaviour in different environments, including the influence of temperature, electric field, solvents and metal salt concentrations, is vital for the design of new ILs and new electrolytes. Moreover, ILs can also promote the interfacial ion transportation in the coming solid-state battery era.

ILs and green hydrogen

The full hydrogen energy chain includes hydrogen production, storage and utilization. Due to the unique properties of hydrogen, hydrogen research has received increasing attention from researchers, realizing applications in several fields. In our previous review article,[49] the production of hydrogen from electrolytic water, hydrogen storage and use of hydrogen in fuel cells based on electrocatalyst preparation, electrocatalytic interface modification, and electrolyte were summarized in detail. Additionally, Nasri *et al.*[50] mainly introduced the application of ILs as nanocatalysts for hydrogen generation and storage. Le *et al.*[51] provided an overview of hydrogen energy production and storage technologies, including an analysis of the economics and challenges; however, ILs were not considered. Therefore, this work is mainly focused on the important application of ILs in the preparation of proton exchange membranes (PEMs) for fuel cells.

In addition to catalysts, a major obstacle in the widespread use of fuel cells is progress in the development of PEMs. Effective hydrophilic clustering within membranes and their high water absorption are crucial for enhancing the proton diffusion in fuel cells. These membranes serve dual roles as electrolytes and electronic insulators, mitigating the risk of electron transfer and short circuits within the fuel cell. During this process, protons transition between different protonic forms, such as H^+ and H_3O^+, as they traverse the membrane. Accordingly, ensuring high proton conductivity is of paramount importance for PEM materials.

In the early stages of the development of proton exchange membranes fuel cells (PEMFCs), significant challenges such as high costs and limited durability were encountered, primarily stemming from the utilization of membranes composed of sulfonated polystyrene–divinylbenzene copolymers. Nevertheless, the progress made in the 1970s brought about the emergence of membranes based on perfluorosulfonic acid, marketed commercially under the brand name Nafion®.[52,53] However, despite these advancements, the challenges and constraints posed by the fluorine content in Nafion membranes, coupled with their associated high cost, have hindered the wider industrial application of Nafion in PEMFCs.[54–59] As a result, various strategies and novel membrane materials are being explored to overcome the aforementioned limitations of Nafion to achieve specific goals.[59,60]

Extensive research in recent decades has focused on composite membranes, aiming to enhance the performance of PEMs and tackle practical challenges (Table 1). The assessment of the fuel cell efficiency relies heavily on ionic conductivity, which is closely intertwined with the characteristics of polymer electrolyte membranes. From a theoretical standpoint, membranes are deemed reliable when their conductivity exceeds 0.01 S cm^{-1}, often benchmarked against commercial Nafion membranes. Lately, significant research efforts have been directed towards exploring the application of ILs as membrane electrolytes in fuel cells.[61–66] The proton conductivity of these IL matrix exchange membranes essentially meets the basic requirements of fuel cells.

The physical and chemical characteristics of ILs can be further optimized through blending with both organic substances, such as amino acids, alcohols, and lipases, and inorganic compounds such as phosphates, citrates, and sulfates.[67–69] PEMs have been tailored to improve the self-humidification, enable higher operational temperatures, reduce the electro-osmotic resistance, and enhance the mechanical and thermal durability of membranes, all while preserving their proton conductivity. Additionally, the integration of solid inorganic materials as proton conductors has been explored to enhance the proton conductivity, and efforts were devoted to developing PEMs with sustained high water retention capacity, while exhibiting slow drying characteristics. Chen *et al.* enhanced the interface between the electrolyte membrane and the catalytic layer by applying a phosphoric acid (PA) coating to a gas diffusion electrode. This intervention effectively lowered the ohmic resistance, resulting in an improved fuel cell performance.[68] At 20% relative humidity and 200 °C, the peak power density reached the

Table 1 IL-based composite membranes applied in fuel cells with several of their properties highlighted

Composite membrane	Ionic conductivity (S cm^{-1}), temperature (°C)	Power density (mW cm^{-2}), temperature (°C)	Mechanical strength (MPa)	OCV (V)	Ref.
Matrimid/[TEA][TfO]	0.02, 130	—	202	—	66
PBI/[dema][TfO]	0.02, 160	29.64, 140	—	1.1	65
OPBI/IL-modified silica	0.24, 160	—	—	—	64
SPEEK/SiO_2-7.5/[bmim][BF_4]-50	0.015, 200	—	—	—	63
Nafion/[TEA-PS][HSO_4]	1.59, 80	200, 100	—	0.92	61
Matrimid/imidazolium-based IL	0.02, 150	—	—	—	62
$CsH_5(PO_4)_2$-PBI	0.026, 200	554, 200	80	1.0	68
XSPEEK/SPBI/PrSGO	0.17, 90	820, 80	1056.76	1.0	67
OPBI–50PI-COOH	0.089, 160	463, 160	—	0.92	70
PBI–Fe_2TiO_5	0.078, 180	380, 180	—	0.86	71
AmPBI-PIL-X-MXeen-3	0.093, 180	219, 180	11.1	0.94	72
ABPBI/5IL@HNTs	149.28, 80	219, 80; 380, 160	>75	0.9	73
UIO-66-NH_2@OPBI	0.169, 160	728.56, 160	35.47	0.95	74
CBOPBI@MOF50%-IL30	0.135, 160	736, 160	—	0.88	75
bPBI-2	0.05, 170	100, 160	11	0.82	76

Matrimid/[TEA][TfO]: Matrimid/triethylamine trifluoromethanesulfonate; PBI/[dema][TfO]: poly(benzimidazole)/diethylmethylammonium trifluoromethanesulfonate; OPBI/IL-modified silica: poly(4,4′-diphenylether-5,5′-bibenzimidazole)-modified silica; SPEEK/SiO_2-7.5/[bmim][BF_4]-50: sulfonated poly(ether ether ketone)/mesoporous silica-7.5/1-butyl-3-methylimidazolium tetrafluoroborate-50; Nafion/[TEA-PS][HSO_4]: Nafion/3-triethylammonium propane sulfonic acid hydrogen sulfate; Matrimid/imidazolium-based IL: Matrimid/1-butylimidazolium bis(trifluoromethylsulfonyl)imide; $CsH_5(PO_4)_2$-PBI: $CsH_5(PO_4)_2$-doped polybenzimidazole; XSPEEK/SPBI/PrSGO: cross-linked sulfonated poly(ether ether ketone)/sulfonated poly(benzimidazole)/propylsulfonic acid-functionalized graphene oxide; OPBI–50PI-COOH: basic polybenzimidazole–50% acidic carboxyl-containing polyimide; PBI–Fe_2TiO_5: polybenzimidazole–Fe_2TiO_5; AmPBI-PIL-X-MXene-3: amino polybenzimidazole-polymeric ionic liquids-X-MXene-3; ABPBI/5IL@HNTs: poly(2,5-benzimidazole)/5% diethylmethylammonium trifluoromethanesulfonate@halloysite nanotubes; UIO-66-NH_2@OPBI: zirconium 1,4-dicarboxybenzene metal organic frameworks-NH_2@poly(aryl ether benzimidazole); CBOPBI@MOF50%-IL30: cross-linked-poly[2,2′-(*p*-oxydiphenylene)-5,5′-benzimidazole]@50% metal organic frameworks-30% (1-butyl-3-methylimidazolium bistrifluoromethylsulfonylimide); bPBI-2: block polybenzimidazole-20% phosphotungstic acid-(1-ethyl-3-methylimidazolium) bis(trifluoro-methylsulfonyl).

maximum of 554 mW cm^{-2}. The results from the durability test of the membrane electrode assembly showed its stable performance under humid conditions but it exhibited a gradual decline in performance in a dry environment. Chattopadhyay *et al.* pioneered the development of advanced fuel cell membranes by integrating cross-linked SPEEK composite membranes with propylene sulfonated-functionalized graphene oxide (PrSGO) and sulfonated polybenzimidazole (SPBI), resulting in an enhanced fuel cell performance.[67] The nanocomposite membranes comprised of XSPEEK/SPBI/PrSGO demonstrated exceptional proton conductivity, reaching 0.17 S cm^{-1} at 100% relative humidity and 90 °C. This attribute translates to an impressive fuel cell performance, achieving up to 820 mW cm^{-2} under fully humidified conditions.

Even with reduced levels of phosphoric acid, the composite membrane maintained substantial proton conductivity. The cohesive hydrogen bond network formed between OPBI and PICOOH within the acid–base composite membrane facilitated proton transfer, thereby facilitating high proton conductivity.[70] Comparatively, the OPBI–50PI-COOH acid–base composite membrane, despite its lower uptake at 109%, demonstrated a remarkable performance, achieving a power density of up to 463 mW cm^{-2} and a proton conductivity of 89 mS cm^{-1} at 160 °C without requiring humidification. Similarly, under non-humidified conditions, the PBI–Fe_2TiO_5 nanocomposite membranes achieved a power density of 380 mW cm^{-2} and a current density of 760 mA cm^{-2} at 0.5 V and 180 °C. This was accomplished with the highest recorded acid uptake at 156% and a proton conductivity of 78 mS cm^{-1} at the same temperature.[71] To achieve a proton exchange membrane with enhanced stability, Wang *et al.*[72] developed a cross-linked composite membrane, AmPBI-PIL-X-MXene-3, with a poly ionic liquid (PIL) as the crosslinking agent and added MXene. Among them, the imidazole ring is connected by hydrogen or ion bonding, and thus the PIL cross-linked films not only improved the conductivity, but also significantly increased the tensile strength. Meanwhile, the introduced MXene surface contained a large number of hydroxyl groups, which also synergistically enhanced the proton conductivity.

The proton conductivity of PEMs containing phosphoric acid and polybenzimidazole increases with an increase in phosphoric acid doping. However, excessive acid doping can result in the degradation of the mechanical strength, dimensional stability, and chemical integrity of the membranes due to the plasticizing effects of free phosphoric acid and the dissolution of polybenzimidazole. It was discovered that halloysite ionogels (IL@HNTs), serving as innovative proton carriers, could effectively substitute free phosphoric acid within the polybenzimidazole membrane.[73] Due to the integration of IL@HNTs, these composite membranes demonstrated remarkable enhancements. They exhibited exceptional proton conductivity (>10 mS cm^{-1}) even at an ambient temperature of 180 °C, while also showing significantly bolstered mechanical strength (>75 MPa), as well as improved water and phosphoric acid absorption capacities. The ABPBI/5IL@HNT composite membrane exhibited the maximum power generation

of 219 and 380 mW cm^{-2} under anhydrous conditions at 80 °C and 160 °C, surpassing that of the phosphoric acid-doped ABPBI membrane by 1.9 and 2.1 times, respectively. The findings suggest that incorporating innovative ionogels in the fabrication of proton exchange membranes with a wide temperature range can address the constraints posed by conventional low- and high-temperature membranes, thereby expanding the operational temperature range of current PEMFCs.

Another effective pathway to achieve ionic conductivity is the combination of an inorganic framework with organic polymers. Through molecular hybridization, inorganic components are incorporated in the organic polymer matrix, resulting in an organic–inorganic composite membrane. This hybrid structure combines the desirable attributes of mechanically and thermally robust inorganic frameworks with the distinct chemical reactivity and advantageous inherent properties such as ductility, flexibility, and processability of organic polymers. This integration effectively overcomes the constraints associated with pure polymer membranes. Wang *et al.*[74–76] prepared composite membranes using metal–organic frameworks (MOFs) and examined how the stability and state of MOFs affect the performance of high-temperature proton exchange membranes. When soaked in phosphoric acid at 160 °C, the MOFs underwent a process where metal ions detach from the ligand and dissolve, leaving the ligand intact within the membrane and leading to the formation of continuous nanopores.[74] These ligands facilitate proton transport within the membrane, contributing to the construction of proton transport pathways. The UiO-66-NH_2@OPBI composite demonstrated impressive proton conductivity of 0.169 S cm^{-1}, despite its thin thickness of just 73 μm. Moreover, it attained a remarkable peak power density of 728.56 mW cm^{-2} under anhydrous conditions at 160 °C. Despite the disruption of the crystal structure in the MOFs, their dissolution resulted in the formation of continuous nanopores, facilitating the absorption and retention of phosphoric acid. This retention, together with the synergistic effect led to an enhancement in the cell performance of the high-temperature proton exchange membranes.

ILs and solar cells

In the past ten years, perovskite solar cells (PSCs) have attracted global attention due to their high efficiency, low cost, simple technology, short industry chain, *etc*. Presently, a consistent and significant ongoing global endeavor is to enhance the efficiency and stability of PSCs for their industrialization.[77] The record power conversion efficiency (PCE) of PSCs has reached 26.10%, which is a remarkable advance compared with its initial value of 3.8% in 2009.[78] However, the challenges related to the degradation of perovskites induced by moisture and long-term photo-instability need to be resolved. Correspondingly, several efficient strategies have been adopted such as optimizing the crystallinity of perovskite films, engineering the electron transport layers (ETL)/hole transport layers (HTL) using ILs, and formation of an efficient passivation layer.[79] Among them, the introduction of ILs shows potential for significant advancements.[80,81] As a result of their inherent qualities, ILs have found practical utility across a wide range of applications, contributing to enhancing the PCE and stability of PSCs.[82] The reports in the literature substantiate that the incorporation of ILs plays diverse roles in the fabrication and functioning of PSCs[83] (Fig. 2).

ILs as additives in PSCs. Various studies have broadly scrutinized the presence of additives or solvents in the perovskite precursor solution, aiming to ascertain their potential impact on both the crystal growth and film morphology of perovskites. In this context, ILs, which are characterized as environmentally friendly additives, have provided a well-established history of promising results in engineering perovskite precursor solutions. Their application is acknowledged to effectively regulate the crystallization kinetics and surface properties. The addition of ILs can delay rapid crystallization, increase the boiling point, and reduce the vapor pressure during the fabrication of perovskite films. These combined effects collectively enhance the quality of PSCs.[84] Wu *et al.*[85] employed the IL of 1-ethylamine hydrobromide-3-methylimidazolium hexafluorophosphate as an additive to $CH_3NH_3PbI_3$ precursor solutions. They discovered that the $ILPF_6$ additive can inhibit the nucleation of $CH_3NH_3PbI_3$, which is ascribed to the establishment of N–H···I hydrogen bonds between the ammonium cations of IL and I^- within the PbI_6^{4-} framework. Consequently, the introduction of IL facilitated uniform nucleation in the perovskite, resulting in an improvement in the PCE achieved for IL-modified devices from 10.08% to 13.01%.

ILs can interact with perovskites *via* hydrogen bonding, chelation, or creation of intermediates, thereby delaying the rapid

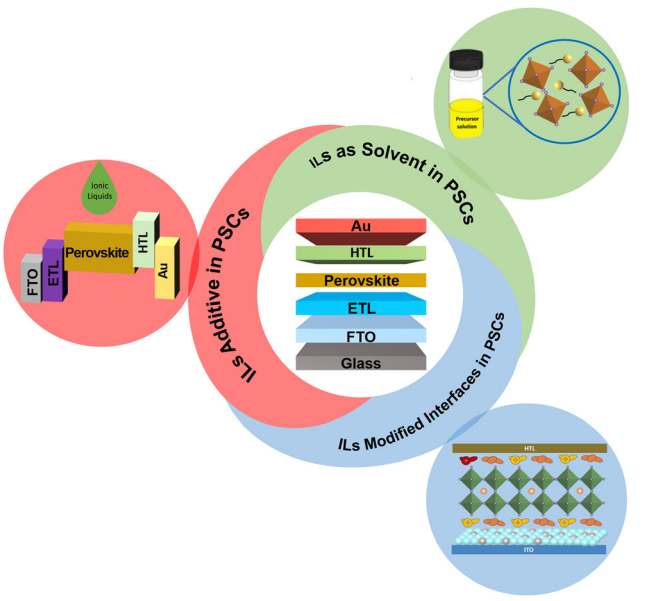

Fig. 2 Graphical illustration of the application of ILs in PSCs.

crystallization of perovskite crystals.[86] Abate *et al.*[87] employed methylammonium formate (MAFa) IL as an additive in the perovskite precursor solution for regulating the perovskite crystal growth. They found that during the perovskite crystallization growth procedure, the initial intermediates were formed by the interaction of $HCOO^-$ and Pb^{2+}. Subsequently, by annealing, I^- gradually replaced $HCOO^-$, eventually leading to the complete displacement of the $HCOO^-$ anions by I^- ions, and thereby impeding the crystal growth. As a result, the PSC device modified with the MAFa additive exhibited a significant PCE of 19.5%. Additionally, in a recent investigation, we utilized an amine-functionalized IL (1-aminopropyl imidazolium bis(trifluoromethyl sulfonyl)imine, $APMImNTF_2$) as a multifunctional additive in the perovskite material to govern the crystallization kinetics of the resulting perovskite film.[88] The microscopic examination of the underlying mechanism disclosed that the $APMImNTF_2$ IL additive created a robust interaction with both Pb^{2+} cations and X^- anions within the perovskite crystals, thus enhancing the crystallization process and imparting hydrophobic characteristics to the modified perovskite film.

ILs can enable Ostwald ripening, wherein tiny grains dissolve while larger grains continue to grow, eventually leading to an augmentation in the average crystal size.[89] In this context, Hu *et al.*[90] employed the MAFa IL as an additive in the precursor solution using a two-step technique. The substantial increase in the average grain size (from 319.1 nm to 798.0 nm) achieved was attributed to the Ostwald ripening effects and reduction in the activation energy for grain boundary migration. Consequently, the PCE of the modified PSC device increased from 21.26% to 23.11%. Similarly, Akin *et al.*[91] introduced 1-hexyl-3-methylimidazolium iodide (HMII) IL as an additive in the precursor solution of formamidinium lead iodide ($FAPbI_3$). This inclusion of the HMII additive promoted the coarsening of $FAPbI_3$ crystals due to its high polarity and boiling point. In addition, the incorporation of the HMII additive established a liquid phase between adjacent grains, effectively lowering the activation energy for grain boundary migration, and thereby facilitating the formation of micron-sized grains. Consequently, the PCE of the PSCs exhibited a notable enhancement, increasing from 17.1% to 20.6%. According to the above discussion, it can be concluded that the incorporation of IL-additives with different functional groups can interact with perovskites *via* hydrogen bonding, chelate bonds, and formation of intermediates, thus leading to an enhancement in the average grain size, passivation of the intrinsic defects, and improvement in the quality of perovskite films by delaying nucleation, retarding crystal growth, and impeding recrystallization.

ILs as green solvents in PSCs. Investigation of state-of-the-art solvents for the fabrication of PSCs is another substantial aspect of recent research endeavors. A diverse range of solvents has been examined for the fabrication of PSCs. However, the combination of dimethylformamide (DMF) and dimethyl sulfoxide (DMSO) is commonly applied to retard the crystallization process, thus leading to the formation of films with improved device performance due to their smooth and compact characteristics. However, a limitation linked with these solvents is the unintentional creation of plumbate intermediates, having an adverse impact on the final film features. Therefore, it is necessary to discover alternative solvent systems.[92] ILs are considered comprehensive substitutes for traditional solvents in solvent modification due to their noteworthy characteristics, including remarkable thermal and electrochemical properties.[93]

Hui *et al.*[94] reported the production of high-quality α-$FAPbI_3$ perovskite films by employing an IL solvent composed of $[MA]^+$ and $[Fa]^-$. Instead of the single-step approach, a two-step technique was adopted. Initially, the precursor solution of PbI_2 was formulated in $[MA]^+[Fa]^-$ solvent, resulting in a distinct light-green color, in contrast to the typical dark-yellow color observed for PbI_2 solutions in DMF/DMSO. This color variation was ascribed to the increased chemical interaction between $[MA]^+[Fa]^-$ and PbI_2, enabled by the N–H···I hydrogen bonds and C double bond O···Pb chelation. This intricate interaction was beneficial, promoting the upright growth of PbI_2 on the substrate. Subsequently, during the stepwise deposition, the unique microstructure of the PbI_2 film processed within these ILs facilitated the incorporation of FAI. This integration results from notably low trap density (4.74×10^{15} cm^{-3}), attributed to the formation of a reduced charge barrier. Consequently, the perovskite film devices fabricated with methylammonium acetate (MAAc) as the solvent demonstrated a remarkable PCE exceeding 23%. Gu *et al.*[95] utilized various IL solvents, specifically MAAc, MAP, and methylammonium isobutyrate (MAIB), to investigate the impact of steric hindrance on the chemical interaction between ILs and PbI_2 in the solution. Liquid-state ^{13}C NMR measurements revealed that the relative shift of the carbon atom in the carboxylate group followed the sequence of MAAc ($\Delta\delta$ = 0.452 ppm) > MAP ($\Delta\delta$ = 0.257 ppm) > MAIB ($\Delta\delta$ = 0.231 ppm), signifying a diminishing interaction between the ILs and PbI_2 with an increase in steric hindrance. A robust IL–PbI_2 interaction can slow down the process of crystallization and enhance the quality of the perovskite film. However, it is less beneficial for solvent removal. Consequently, the MAP-modified device displayed a superior photovoltaic performance, attaining a PCE of 20.56%. According to previous reports, there are several reasons supporting the enhancement in perovskite film quality through the utilization of ILs as solvents. Firstly, ILs can enable the formation of a favored crystal orientation *via* covalent binding. Secondly, the interaction between ILs and perovskites is characterized by a diminished chemical interaction strength, thereby leading to an augmentation in the size of the micelles within precursor solutions. Thirdly, the elevated boiling points characteristic of ILs enables a residual quantity to persist within perovskite films, thereby significantly passivating the defects.

IL-modified interfaces in PSCs. Due to their exceptional chemical structures, the integration of ILs in various com-

ponents of PSCs has attracted significant interest in subsequent years. Prior research indicated that ILs exhibit robust interactions with perovskite materials, having a notable impact on the electrical, optical, and morphology characteristics of the devices.[96] In this section, we scrutinize the recent and innovative studies focused on the addition of ILs in the top surface of the perovskite. In the context of both cell architectures of n–i–p- and p–i–n-type PSCs, their performance is constrained by the presence of an elevated defect density and deprived interface contacts at both the buried and upper interfaces. Thus, to address these restrictions, a variety of ILs has been employed as interface modifiers to enhance the quality of perovskite films, mitigating defects and augmenting the carrier transport properties.[97]

Tang *et al.*[98] presented the use of the 1-butyl-2,3-dimethylimidazolium chloride ([BMMIm]Cl) IL for passivating surface defects in HTL-free PSCs. They found that the electron-rich nitrogen atom within [BMMIm]Cl not only facilitated the passivation of uncoordinated Pb^{2+} and Cs^{+} ions but also reduced the work function of the perovskite to close to that of the carbon electrode. In addition, the hydrophobic alkyl side chain in [BMMIm]Cl promoted the hydrophobic nature of the perovskite films. Consequently, the PCE of the IL-modified device exhibited an improvement from 6.15% to 9.92%, and it maintained 98.5% of its initial PCE even in an ambient atmosphere at 20 °C with 70% relative humidity for 30 days, without further encapsulation. Similarly, Liu *et al.* employed the IL methyltrioctyl ammonium trifluoromethane sulfonate (MATS) to the passivate traps and boundaries located at the interface of the i–n junction.[99] The perovskite surface treated with MATS displayed enhanced smoothness and improved interaction with the ETL, leading to an increase in PCE from 11.21% to 16.10%.

In n–i–p type PSC devices, TiO_2 is frequently employed as an ETL. Unfortunately, the device performance is restricted due to the inherently low electron mobility and elevated electronic trap density of TiO_2.[79] In this case, Shi and co-workers[100] observed that the application of a precoating of MAAc on the TiO_2 layer led to an enhancement in the quality of $CsPbIBr_2$ films. This improvement was attributed to the uniform distribution of methylammonium cations (MA^{+}), serving as nucleation centers, thereby reducing the potential barrier for the formation of the α-phase perovskite. Consequently, the PCE of the devices modified with MAAc increased from 6.42% to 8.85%. In contrast to TiO_2, the SnO_2 ETL exhibits elevated electron mobility, enhanced stability under ultraviolet (UV) light exposure, and a comparatively reduced processing temperature. Gao *et al.*[101] introduced buried interface modulation engineering by incorporating 4-fluoro-phenylammonium tetrafluoroborate ($FBABF_4$) IL. $FBABF_4$ simultaneously enhanced the perovskite crystallization kinetics and caused interfacial defect passivation and energy band alignment. Subsequently, the device modified with $FBABF_4$ demonstrated a PCE of 23.07% and maintained 85% of its initial PCE under conditions of 35% ± 5% relative humidity in the absence of light for 3000 h. In summary, it can be concluded that ILs play a significant role in the modification of the top and buried surface of PSCs by mitigating defects, enhancing the crystallization of perovskites and augmenting the transport of charge carriers. Remarkably, ILs can regulate the PbI_2 at the upper interface, establishing stable complexes that contribute to the efficiency and stability of PSCs.

In PSCs, ILs have been extensively utilized to enhance their efficiency and stability through various means, such as defect passivation, regulating their crystallization kinetics and energy level, and enhancing their charge transport abilities. The incorporation of ILs as additives is promising in regulating the crystallization dynamics of perovskite materials. Their utilization displays the capability to facilitate the growth of larger perovskite crystals and the realization of more homogeneous perovskite films. However, the distribution of ILs within the system and their corresponding mechanism need to be investigated in detail given that they play a pivotal role in their function of defect passivation, work function modulation, and inhibition of ion migration. ILs can be deployed as the sole solvent or in combination with conventional solvents such as DMF and DMSO. This effectively retards the crystallization process, facilitating the formation of high-quality perovskite films characterized by a uniform large grain size and compact structure. Furthermore, ILs can be incorporated into the top and buried interface of perovskites. As the top passivation layer, they interact with perovskites to form complexes, which significantly enhance the PCE and stability of the cell. Alternatively, in the buried interface, ILs play a pivotal role in modulating the hydrophobicity of the substrate, thereby facilitating the formation of perovskite films with enhanced quality.

IL acceleration to develop valuable electronic materials

ILs and 2D electronic materials

The development scale and technical level of the electronic material industry (EMI) have become an important symbol for measuring the scientific progress and national defense strength of a country. Therefore, the EMI occupies an important strategic position in the national economy. Unarguably, EMI has become the most intense technological innovation and international competition in the materials field (such as integrated circuits and semiconductor junctions).[102,103] High-end electronic materials, as the basis and core of integrated circuits, new displays, and 5G communications, have become the commanding heights pursued by all countries. However, the preparation of electronic materials with the necessary characteristics has restricted the rapid development of EMI.[104] For example, achieving the synthesis of two-dimensional (2D) electronic materials at the wafer scale and transfer them from

the substrate cleanly and without loss. Also, removing the residue without destroying the 2D material structure during the subsequent photolithography, deposition, and other processes, which affects the performance of the device. The emergence of ILs opens up a new avenue to solve the above-mentioned problems due to their unique properties, witnessing great advancement in the exploration and development of electronic materials (the roles and applications of ILs in the field of electronic materials are shown in Fig. 3). In this section, the bottlenecks in EMI are highlighted and classified. Further, the roles and applications of ILs in EMI, including integrated circuits (IC) and semiconductor junctions, are summarized and discussed.

Integrated circuit (IC) technology, as an irreplaceable driving force of the fourth industrial revolution, has aroused a "gold rush" and became the focus of the pursuit of countries. During the age of large data sets, even more sophisticated electronic gadgets are required to manage the enormous volume of data quickly. However, further shrinking the sizes of silicon transistors to increase the chip integration density has become prohibitively expensive. Also, in some cases, the above-mentioned issue has encountered the limits of Moore's law.[105,106] In addition, the development of cutting-edge electronics from conventional rigid to foldable/flexible/rollable devices has unique challenges. Thus, the development of electronic devices with lighter weight, greater durability, and more space efficiency has become a challenge in the upcoming generation of electrical and optoelectronic equipment.[107,108]

As mentioned above, the development of high-powered electronic materials is an essential prerequisite for obtaining pioneering equipment. Therein, nanoelectronics based on heterostructures of 2D materials have been regarded as the most promising candidates for next-generation high-performance computational technology.[109,110] However, all 2D materials suffer the difficult transition from micron-sized thin sheets to single wafer scale, limiting their industrial applications. Accordingly, numerous studies have focused on the development of high-quality wafer-scale single-crystal thin films and two main principles have been refined and proposed, as follows:[111–113] (I) a low nucleation density to ensure sufficient growth space and (II) controllable oriented growth to achieve defect-free single crystals.

Based on these two principles, innovative theories have been developed. Briefly, two distinct recapitulative strategies have been developed for the synthesis of high-powered electronic materials (Fig. 4a). One is the top-down method, involving the exfoliation of bulk 2D wafer-scale materials into dispersed nanosheets. The other is based on bottom-up assembly, in which high-powered electronic materials can be prepared by controlling the process of nucleation and growth on the specific liquid surface. Both strategies have been widely applied for the preparation of high-powered electronic materials with the desired functions.

In the case of the top-down strategy, the lack of high-efficiency dispersants and exfoliation agents has become a bottleneck in developing electronic materials with the necessary characteristics. Fortunately, task-specific ILs possess high dielectric constants, which provide shielding effects to prevent stacking interactions due to van der Waals interactions, further contributing to the efficient dispersion of nanomaterials.[114,115] Therefore, ILs as excellent solvent media for the exfoliation and stabilization of 2D materials have become a research hotpot in the field of electronic materials. For example, 2D wafer-scale graphene prepared by the chemical vapor deposition (CVD) method has been regarded as one of the most promising materials applied in the IC industry.[116] However, appropriate catalysts are necessary and a graphene film grown on a solid substrate cannot be transferred to another substrate for further use, limiting the purity of the final products. In this case, ILs have surface tensions closely matching the surface energy of graphite, creating a new path for the direct exfoliation of graphite.[117,118] Aldroubi *et al.*[118] developed thin few-layer graphene sheet dispersions with long-term stability and high concentration (*ca.* 3.6 mg mL^{-1}) by the strategy of sonochemical exfoliation, while using aromatic imidazolium-based ILs as an exfoliation agent (Fig. 4b). They suggested that the ILs can achieve the exfoliation of graphite through π–π and cation–π interactions.

Similarly, monolayer molybdenum disulfide (ML-MoS_2), as an emerging 2D semiconductor showing potential for use in flexible integrated circuits (ICs), has also been obtained by using ILs as exfoliation agents.[119,120] Liu *et al.*[120] studied the influence of altering the cationic and anionic combination of ILs on the exfoliation of 2D MoS_2. They proposed a correlation between the intermolecular interactions of the IL components and their ability to exfoliate MoS_2 nanosheets. Intermolecular associations in the form of molecular networks play a crucial role in the intercalation and exfoliation of ILs (the interaction between different ILs and MoS_2 nanosheets shown in Fig. 4c). In addition, ILs have also been used as exfoliation agents to obtain 2D electronic materials using other materials, such as WSe_2 and h-BN, which can act as channel materials in field-effect transistors (FETs).[121–123]

In the case of bottom-up fabrication, the core of this strategy is controlling the process of nucleation and growth. For example, Xu *et al.*[124] developed a general "solution epitaxy" strategy to control the crystal growth and obtained high-quality two-dimensional crystal organic semiconductors (2DCOS) (Fig. 4d). In this process, molecular materials were added to the surface of water (or another solvent), and then the mole-

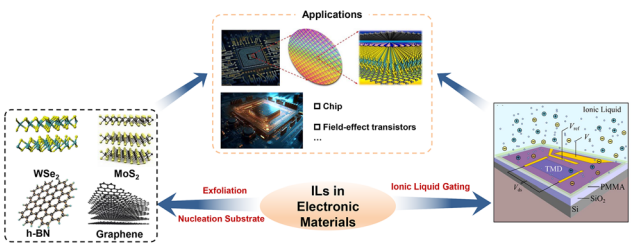

Fig. 3 Roles and applications of ILs in the field of electronic materials.

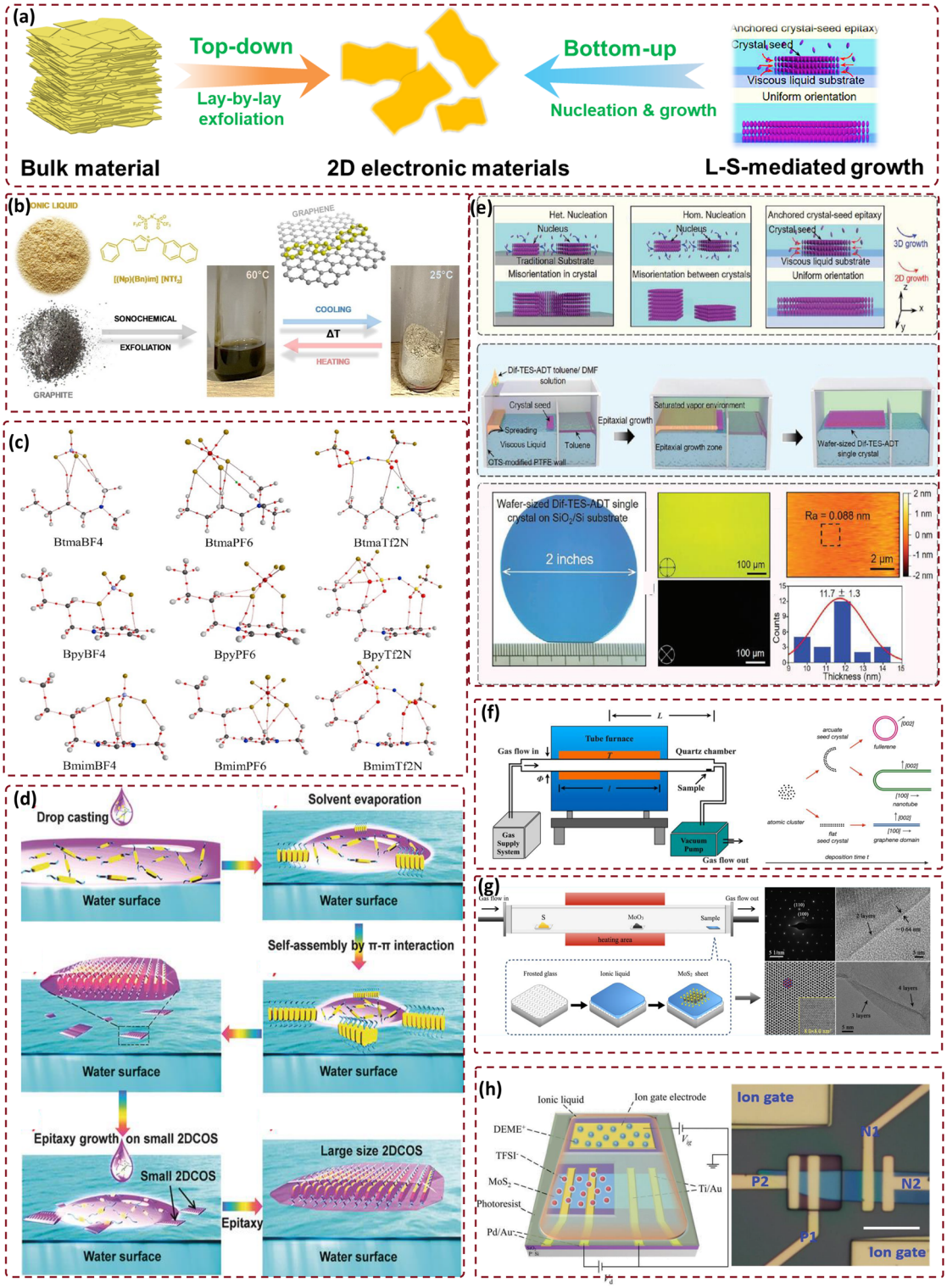

Fig. 4 Schematic illustration of (a) top-down and bottom-up synthetic strategies for 2D electronic materials. (b) Process of sonochemical exfoliation using aromatic imidazolium-based ILs as exfoliation agents.[118] Reproduced from ref. 118 with permission from Elsevier, copyright 2023. (c) Interaction between different ILs and the MoS_2 nanosheet.[120] Reproduced from ref. 120 with permission from Elsevier, copyright 2020. (d) Growth of 2DCOS by the strategy of "solution epitaxy".[124] Reproduced from ref. 124 with permission from Wiley, copyright 2016. (e) Wafer-scale growth of 2D organic semiconductor single crystals by the strategy of anchored crystal-seed epitaxial growth and corresponding properties.[112] Reproduced from ref. 112 with permission from Wiley, copyright 2023. (f and g) Growth mechanism of two-layered allotropes of carbon and single- to few-layered MoS_2 sheets by the strategy of LP-CVD.[129,130] Reproduced from ref. 129 and 130 with permission from Elsevier, copyright 2022 and ACS, copyright 2023, respectively. (h) Structure of a four-electrode MoS_2 transistor and optical micrograph.[131] Reproduced from ref. 131 with permission from Wiley, copyright 2023.

cular materials dispersed quickly over the whole water surface through surface tension. The molecules formed aggregates gradually through strong π–π interactions, changing into micrometer-sized 2DCOS, that which further act as seed crystals for the epitaxial growth of small 2DCOS. Finally, 2DCOS with sizes on the millimeter scale or even over a centimeter were obtained. Based on this, Wang *et al.*[112] achieved the wafer-scale growth of 2D organic semiconductor single crystals by the strategy of anchored crystal-seed epitaxial growth (Fig. 4e). In this strategy, the multiple nucleation behaviors of the molecules were suppressed due to the intentional introduction of crystal seeds. Consequently, wafer-sized few layer bis(triethylsilythynyl)-anthradithphene organic single crystals were successfully fabricated. All these studies indicate that the appropriate liquid solvent environment with suitable surface tension can guarantee the organic solution spreading on the as-built surface, enabling the formation of few-layer or even monolayer organic crystals.

As mentioned above, the surface tension of ILs can be finely tuned due to the designability of their structure.[125,126] Therefore, ILs and their analogues as structural regulators to tune the behavior of nucleation and growth have been widely used in various fields.[127,128] Similarly, ILs also exhibit huge potential in the synthesis of electronic components. Employing LP-CVD, Shen *et al.* produced single- to few-layered graphene and its allotropes (including single- to multi-wall nanotubes and nested closed fullerenes) on the surface of ILs at room temperature in the absence of metallic catalysts (Fig. 4f).[129] They suggested that the pristine properties of the seed crystals on the IL substrate can be tuned, further influencing the final species of the allotropes. Shen *et al.* developed single- to few-layered MoS_2 sheets with an average size in the order of micrometers on an IL surface in a similar manner (Fig. 4g).[130] In this process, the ILs provide a quasi-free sustained substrate with isotropic characteristics and quasi-atomic surface smoothness. In this case, the deposited atoms and seed crystals on the surface of the ILs can diffuse randomly, rotate, and align on the liquid surface freely with large diffusion coefficients compared with that on traditional solid substrates, contributing to the efficient formation of patterns and ordered objects. It should be noted that the application of task-specific ILs in electronic components by the method of bottom-up fabrication is still in its infancy and new strategies are triggered with the development of ILs.

In addition to the above-mentioned roles of ILs in electronic materials, the technology of "ionic liquid gating (ILG)" was proposed to construct semiconductor junctions in recent years, which is of great significance for the development of electronic devices.[131–133] For example, a gated device structure consisting of IL exposed parts and photoresist-protected channels was proposed by Chang[131] (Fig. 4h).

The designed IL gated device possessed excellent rectification behavior with a current on–off ratio exceeding 10^6 in both Schottky and p–n junction modes. They suggested that the ILs can induce an ultra-high hole doping density and a p–n junction with a large effective barrier is formed between p-type and n-type MoS_2 with suitable doping level on two sides. Consequently, a device with a rectification ratio greater than 10^6 was obtained. In the future, ILG as an effective tool to enhance the carrier densities will become a promising technique for exploring the electronic phases of materials in extreme doping regimes.

ILs and photolithography for advanced electronic components

As photolithography technology continually evolves, the performance expectations for electronic components escalate, and research into the utilization of ILs has ignited fresh possibilities in this domain. This section offers an overview of the studies exploring the application of ILs in photolithography-based electronic components.

The semiconductor industry has invariably relied on advancements in lithography technology to progressively reduce the dimensions of features in integrated circuits. Extreme ultraviolet lithography (EUV) has been prognosticated as a potential substitute for 193 nm lithography; however, technical and economic issues have impeded its large-scale implementation.[134] Block copolymer (BCP)-directed self-assembly (DSA) is a nanomanufacturing technique employed to mitigate the periodicity of traditional optical methods for patterning. Poly(styrene)-*block*-poly(methyl methacrylate) (PS-*b*-PMMA) is one of the most extensively studied BCPs for direct self-assembly, which is attributed to its outstanding compatibility with traditional processes. However, PS-*b*-PMMA cannot facilitate the patterning of sub-10 nm features due to its low Flory–Huggins interaction parameter (χ_{eff}). Thus, to address this issue, Sunday *et al.*[135] reported the use of ILs ([BMPR][TFSI]) as an additive in PS-*b*-PMMA to augment χ_{eff}. This study probed the influence of ILs on the thickness of the layers and the interface width of BCPs, together with the associated alterations in line edge roughness (LER) in the DSA patterned samples. The findings revealed that the introduction of ILs led to a reduction in the interface width and an increase in χ_{eff} within the parallel platelet layers of the BCP, but LER did not invariably decrease. Thus, this established a crucial design criterion for future material systems (Fig. 5a). Chen *et al.*[136] investigated the distribution and interaction dynamics of IL 1-hexyl-3-methylimidazolium hexafluorophosphate (HMHF) within PS-*b*-PMMA BCPs. The segmental dynamics of the rigid, intermediate, and mobile molecular constituents in PS-*b*-PMMA/HMFF were delineated by solid-state nuclear magnetic resonance spectroscopy, revealing that selective interaction occurred between PMMA and HMHF. The surface energy and interfacial behavior of the polymer/HMFF admixture demonstrated that HMHF was preferentially situated beneath the surface of the PMMA matrix. Owing to this distribution, the disordered PS-*b*-PMMA, which had been treated with HMHF, developed vertical sub-10 nm features following thermal annealing (Fig. 5b). The process of demixing HMHF IL additive within PS-*b*-PMMA BCPs was elucidated by an equation that detailed the dependence of the interaction parameter on molecular weight. Hao *et al.*[137] examined the influence of the IL 1-hexyl-3-methylimidazolium hexafluoro-

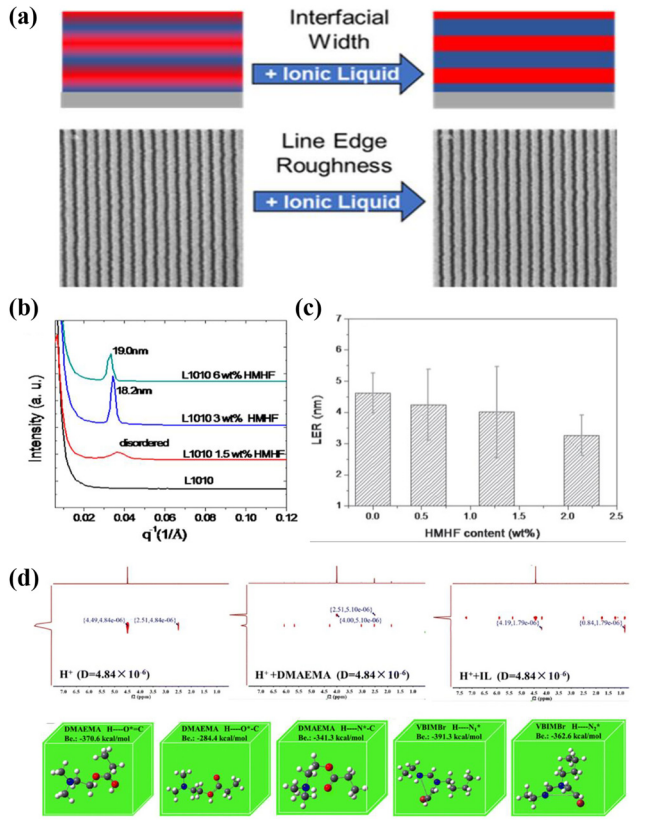

Fig. 5 (a) Influence of IL additives on lithography.[135] Reproduced from ref. 135 with permission from the American Chemical Society, copyright 2020. (b) SAXS diffraction profiles of PS-*b*-PMMA BCP L1010 and its HMHF mixtures with different ratios after annealing at 200 °C for 5 min.[136] Reproduced from ref. 136 with permission from the American Chemical Society, copyright 2019. (c) LER values *versus* HMHF contents in L2222 BCP and HMHF blends.[137] Reproduced from ref. 137 with permission from IOP Publishing, Ltd, copyright 2023. (d) DOSY diffusion-NMR spectroscopy of H^+ mixed with DMAEMA/VBIMBr and optimized interaction structures of DMAEMA/VBIMBr with H^+ at the B3LYP/6-31G (d) level.[138] Reproduced from ref. 138 with permission from The Royal Society of Chemistry, copyright 2023.

phosphate (HMHF) adjuvant on the line edge roughness (LER) performance of PS-*b*-PMMA self-assembled patterns. The findings demonstrated that the inclusion of trace HMHF preserved the lithography compatibility of the PS-*b*-PMMA block copolymer film, elevated the Flory–Huggins interaction parameter (χ) between the two phases, thereby intensifying the phase separation, diminishing the interface width, eradicating defects, and enhancing the LER and pattern transfer fidelity, particularly for low molecular weight (or low χ_N) PS-*b*-PMMA, successfully generating LER of 1.69 nm layer-by-layer array patterns (Fig. 5c). This investigation revealed a promising strategy to overcome the limitations of existing block copolymers. Furthermore, *via* the incompatibility between the comb-like PIL main chain segment and the hydrophobic alkyl chain, the charged connecting group significantly fostered this microphase separation, and structural domains of sub-3 nm were successfully realized, and these organized structures exhibited exceptional thermal stability. The findings of this investigation are anticipated to offer a straightforward and effective approach for generating electronic device templates *via* lithography technology.[139]

Given that photoresist films are typically fabricated *via* spin-coating, they involve the use of not only polymers but also volatile solvents, prompting the quest for a more environmentally benign approach in light of mounting concerns regarding environmental and health-related issues. Capitalizing on the distinctive characteristics of ILs due to their intriguing properties such as low volatility, high ionic conductivity, and excellent thermal stability, Rola *et al.*[140,141] developed a novel material (*i.e.*, room temperature ionic liquid (RTIL) incorporating polymerizable allyl groups) for the fabrication of planar structures. This material is e-beam curable and solvent-free, and the method for fabricating polymer microstructures through e-beam-activated polymerization of RTIL has been meticulously investigated and expounded. The results demonstrated that selective exposure of RTIL films to high-energy electron beams led to their curing. Significantly, these films could be fabricated *via* spin-coating of pure ILs, that is, without the use of any additional solvents, thereby making the process safer and more environmentally benign. Due to the optical properties of polymeric RTILs, they appear to be promising materials for the fabrication of photonic components. Liu *et al.*[138] synthesized photoresists through the copolymerization of 1-butyl-3-vinylimidazolium bromide (VBIMBr) and acrylate. The hydrophilic nature of VBIMBr enhanced the adhesion between the photoresist and the hydrophilic silicon substrates, thereby avoiding the need for hazardous hexamethyldisilazane (HMDS) vapors. The IL-based photoresist could be developed with water instead of the aggressive developer, tetramethylammonium hydroxide (TMAH). Moreover, this study (Fig. 5d) investigated the regulatory mechanism of acid diffusion during the post-baking process, and the ionic-based photoresist exhibited a minimal line edge roughness (LER) and exceptional photolithographic performance in comparison to traditional acrylate photoresists, achieving linear resolutions of 0.5 μm (DUV) and 100 nm (EBL), respectively. Additionally, given the high ionic conductivity and excellent flexibility of ILs, this study integrated them with electrochromic devices. Similarly, Zhang *et al.*[142] took advantage of this property by incorporating 1-ethyl-3-methylimidazolium chloride (EmimCl) in the PVA system to improve the mobility and ionic conductivity of the polymer chain electrodes at both ends of the device.

In summary, ILs, known for their unique physicochemical properties, are highly compatible with photoresists, making them an excellent choice for conventional lithography applications. The potential of this material to directly generate ion-conducting micropatterns and 3D microstructures through conventional lithography represents a promising opportunity. Future research should focus on further optimization and implementation of this material in flexible microelectrochemical devices, including soft robotic actuators.

ILs leading a new era in biotechnologies

ILs creating tunable solvents or cosolvents for biocatalysis

ILs have been employed as tunable solvents or cosolvents for biocatalysis since the third-generation ILs introduced the properties of hydrogen bonds.[143] These ILs are endowed with task specificity, low biotoxicity, and favorable biocompatibility. With the proposed fourth generation of ILs, the synergistic effects of combed ILs with metal or organic salts have broadened their biocatalysis applications. There are many reviews discussing Bio-ILs systems from different perspectives, such as biocompatible ionic liquid (Bio-ILs) synthetic pathway,[149] Bio-IL catalytic mechanisms,[150] Bio-IL degrading factor,[151] Bio-IL interactions in enzymatic catalysis,[152,153] Bio-ILs in different catalytic reactions,[154] Bio-IL enhancements in biomolecules,[155] Bio-IL in producing renewable commodities,[156] and Bio-ILs in pharmaceutical applications.[157,158] Alternatively, a new perspective called ionozyme was proposed by our team for the first time in 2021,[159] where ILs were used as a solvent and enzyme stabilizer, resulting in an increase in the solvation and conversion of CO_2 over formate dehydrogenase (CbFDH). Based on the concept of ionozyme, we presented a review of ILs as tunable solvents and modifiers working in bioacatalysis[144] and a review of the microenvironment of ionozyme converting CO_2 to high-value compounds through biocatalysis.[160] Thus, we focused on the mechanism of IL optimization of biological processes. Furthermore, we elaborate on the biological application of IL from the aspects of how to improve enzyme stability and catalytic activity in this review.

To date, many studies have reported that ILs play a positive role in boosting the performance of enzymes in biocatalysis systems, in which can be influenced by their stability and catalytic efficiency (Table 2). Briefly, ILs can enhance the stability of enzymes by interacting with their structure, affecting the solvent microenvironment, and coating enzymes. Besides, the ILs can promote the enzymatic efficiency by interacting as organic solvents in the system, interacting with enzymes or interacting with the products and substrates. In this section, the mechanism of ILs involved in ionozymes working as stabilizers and activators will be discussed (Fig. 6). The ILs involved

Table 2 Bio-ILs applied in biocatalysis

Bio-ILs	Enzymes	Effect of Bio-ILs	Advantages	Ref.
NIL (amino-modified imidazole IL)	Laccase	Promoting the affinity to hydrophobic substances and the interaction between the carrier and laccase	Higher stabilities in wider range of pH and temperature	161
[BuTr][AA]	Lipase	Formation of weak interaction and reduction of α helix	Biocompatibility of most [BuTr][AA] ILs to lipase was better than [Bmim]Br	162
[GVIM][Cl]	Lipase	Modulating the multisite weak force (MSWF) of the polymers on the active centers	Optically pure product with high conversion (>99%) and ee (>99%) were obtained	163
Imidazolium-based ILs with $[tf_2N]^-$	Lipase	The open formation of lipase was anchored and that the rigidity of lipase was enhanced *via* multiple interactions	2.15 and 1.49 folds higher than that of free PPL and PPL-MPDA, respectively	164
[TMG][OAc] [DBU][Cl]	Xylose	Responsible for catalyzing controlled interactions of amino acid residues	Enhancing the stability of xylose reductase by 10 folds	165
[Emim][OAc]	Cellulase	Positively signifies a gradually increase in amorphism and porosity	Increasing conversion of cellulose by 33.7%	166
[Emim][DEP]	Cellulase	Increasing in surface potential and the hydrophobic groups on the surface	Adsorption capacity could reach 326.04 mg g^{-1} and reusability was improved by 25%	167
[Omim][PF_6]	*Candida antarctica* lipase B	Acting on substrates to increase concentration	5-Fold higher activity than the free enzyme	168
[Bmim][Br] [Bmim][$MeSO_4$]	Chloroperoxidase	Forming new substrate channel	Improve enzyme activity	169
Triethanolammonium butyrate (TEAB)	Urate oxidase	Transforming the random coil into an α-helix and β-sheet	Improving the thermal stability and catalytic efficiency	170
[ProC12][H_2PO_4]	*Candida antarctica* lipase B	α-Helix decreased and β-sheet increased	3 times catalytic efficiency and 2.8 times K_{cat}/K_m	171
[CH][ProCOO] [TMGH][PhOCOO]	Formate dehydrogenase	Facilitating hydride transfer by promoting its relative orientation and forming new hydrogen bonds at the active site		172
[Emim]BF_4	Phenylalanine dehydrogenase	Increasing the solubility of hydrophobic substances and concentration of substrate	Activated enzyme activity by 132%	173
[VHIm][Br], [VEIm][Br]	Carbonic anhydrase	Enhancing the concentration of dissolved CO_2	Improving the catalytic efficiency	148
[EMIM][BF_4]	Lumbrokinase	Improving the solubility of chlorinated organic pollutants and ionic strength of electrolyte	Mass transfer rate constants increase by 6.9 times	174
[Emim]Cl [Ch][Ser]	Lysine decarboxylases	Promoting the protein–ligand complexation	Improving the catalytic activities of [Emim]Cl and [Ch][Ser] by 124.2% and 116.2%, respectively	175

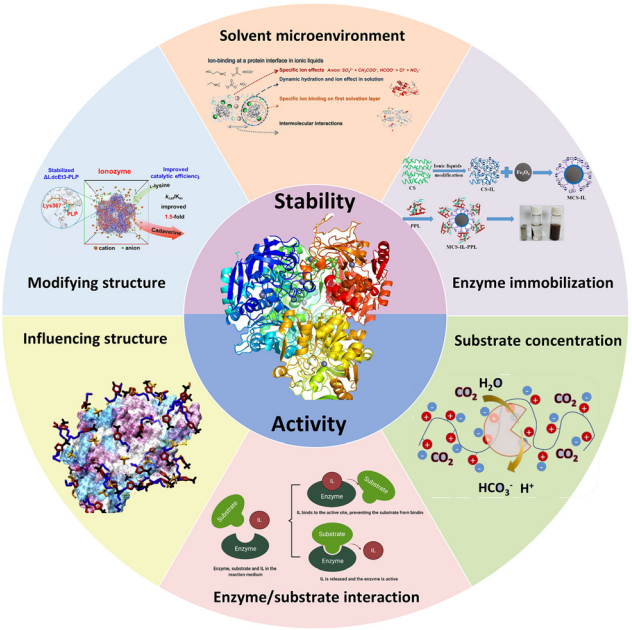

Fig. 6 Approaches for enhancing enzymes using ILs. Methods for improving stability include modifying structure.[144] Reproduced from ref. 144 with permission from Taylor & Francis, copyright 2023; solvent microenvironment.[145] Reproduced from ref. 145 with permission from Elsevier, copyright 2022; and enzyme immobilization.[146] Reproduced from ref. 146 with permission from Elsevier, copyright 2020. Methods for improving activity include influencing structure,[147] enzyme/substrate interaction[147] and substrate concentration.[148] Reproduced from ref. 147 and 138 with permission from Elsevier, copyright 2021 and 2022, respectively.

in stabilizing enzymes can be categorized based on three aspects, as follows:[176–178] (1) stabilizing enzymes by modifying the structure of ILs, where functionalized ILs can endow enzymes with greater stability. It can be observed that the hydrophobic chain of ILs can help stabilize enzymes, while their hydrophilic parts may destroy the enzyme.[179,180] Qiu *et al.*[161] investigated an amino-functionalized IL using dialdehyde starch (DAS) and manufactured an immobilized system named Fe_3O_4-nano-imprinting lithography (NIL)-DAS. Laccase was employed and its stability increased in a wide pH and temperature range. Also, Peng *et al.*[165] carried out a study on tropine-amino acid ([BuTr][AA]) interacting with lipase. The result showed that this IL was more biocompatible because of its physicochemical properties. (2) Stabilizing enzymes by modifying the solvent microenvironment, such as water-in-IL microemulsions,[181] additives,[182] and IL coating.[183] Malla *et al.*[162] proposed the use of *N*,*N*,*N*,*N*-tetramethylguanidinium acetate ([TMG][OAc]) and 1,8-diazabicyclo[5.4.0]undec-7-ene chloride ([DBU][Cl]) as a medium for enhancing the stability of xylose reductase by 10 fold. (3) Stabilizing enzymes by immobilization and attachment, where the immobilization carrier can be MOFs[167] or solid gels[184] and the attachment can be covalent bonding with polyethylene glycol (PEG),[185,186] three-phase partitioning, micro-crystals or lyophilization. Zhou *et al.*[166] reported the synthesis of a polyhydrogel microsphere called poly *N*-isopropylacrylamide (PNIPAM) working in 1-ethyl-3-methylimidazolium acetate ([Emim][OAc]). The system immobilized cellulase by the physical adsorption occurring in its hydrophobic region, resulting in an increase in the conversion of cellulose by 33.7%. Their group also investigated another system in IL (1-ethyl-3-methylimidazolium diethyl phosphate [Emim][DEP]) media,[167] in which the cellulase system could be stabilized *via* zeolitic imidazolate framework (ZIF-8) carriers. The enzyme was immobilized by physical adsorption and the adsorption capacity could reach 326.04 mg g^{-1}. This could increase both the ILs and the enzyme tolerance to the external environment. Overall, Bio-ILs play an important role in constructing ionozyme systems and improving the stability of enzymes.

In addition to the fact that ILs can greatly affect the stability of enzymes, their effect on the catalytic efficiency of enzymes is also an issue worth investigating. Based on the current studies, ILs enhance the activity of enzymes mainly by influencing their microenvironment in the following ways: firstly, ILs affect the enzyme itself by directly or indirectly influencing its structure, including conformation, active pockets, and active sites. Secondly, the catalytic efficiency is enhanced by interacting with the substrates and products by either reacting with them or by altering their partitioning between the aqueous and nonaqueous phases. Finally, increasing the concentration of substrate in the enzyme microenvironment is also an effective method.[187]

The effect of ILs on the structure of enzymes has been widely discussed, which is influenced and regulated by the physical and chemical properties of the solvent, such as polarity, hydrophobicity, hydrogen bond alkalinity, nucleophilicity, and viscosity. In many cases, ILs modulate the structure of enzymes through their hydrophilic and hydrophobic properties to promote their catalytic efficiency. For example, the catalytic pocket is an important structure for enzyme activity, which in many enzymes tends to be closed due to the hydrophobicity of the surface. Wang *et al.*[179,180] formed PILs by free radical co-polymerization with divinylbenzene (DVB) and IL monomers. The hydrophobicity of the PILs contributed to the catalytic performance at the interface of the aqueous and oil phases in the "open" state. Suo *et al.*[188] prepared IL-modified magnetic carboxymethyl cellulose nanoparticles (IL-MCMC) and used them as a carrier for enzyme immobilization. The specific activity of immobilized porcine pancreatic lipase (PPL-IL-MCMC) was 1.43 times and 2.81 times higher, which was achieved by introducing ILs to increase the hydrophobicity of the carrier, thus inducing the lid of the lipase to open. ILs can also impact the secondary structure of enzymes, thus affecting their conformation in different ways. Chen *et al.*[189] reduced the content of α helix in the enzyme structure through ILs, thus enhancing the affinity between the enzyme and the substrate and increasing the catalytic efficiency by 1.48 times. Ghanbari-Ardestani *et al.*[170] studied the effects of tetraethylammonium (TEAB) ILs on the structure and function of urate oxidase (UOX), indicating that TEAB maintained the integrity of the enzyme active site in the system by transforming the random

coil into an α-helix and β-sheet, thus improving the enzyme activity. These structural changes are often achieved through the hydrophobic interaction between ILs, reaction solvents and enzymes, and some directly through electrostatic force and other effects on the enzyme itself. Zhang *et al.*[171] designed an efficient and stable enzyme–metal composite catalyst using mesoporous polymeric liquid as the carrier. The IL binds to the electrostatic charge on the surface of *Candida antarctica* lipase B (CaLB) through electrostatic attraction, and the strength of the binding force can be adjusted by the type and number of ion sites in the carrier. Some ILs can also destroy the original structure and improve the catalytic efficiency through the new structure. Ghorbani *et al.*[169] adopted a low concentration of 1-butyl-3-methylimidazolium bromide ([BMIM][Br]) for the catalysis of chloroperoxidase (CPO), resulting in a new channel, which facilitated the entry of the active site and "heme" into the surface, leading to higher enzyme activity and higher efficiency.

Based on regulating the enzyme structure, some studies focused on promoting the interaction between the enzyme and the substrate, some by enhancing the binding of the enzyme with the substrate and some by promoting the transfer. Zhang *et al.*[190] increased the hydrogen bond between laccase and the substrate through the introduction of an IL, thus strengthening the intensity and frequency of the interaction between the enzyme and substrate. Ji *et al.*[159] reported a new "ionozyme" strategy, achieved by the formation of the key intermediates choline L-prolinate ([CH][ProCOO]) and *N*,*N*,*N*,*N*-tetramethylguanidinium phenol ([TMGH][PhOCOO]). In this process, the distance between nicotinamide adenine dinucleotide (NADH) and CO_2 (3.9 Å) was shortened, facilitating hydride transfer by promoting its relative orientation and forming new hydrogen bonds at the active site. However, the addition of ILs does not promote the binding of the substrate to the enzyme. Stevens *et al.*[191] studied the effect of 1-ethyl-3-ethylimidazolium acetate ([C_2C_1Im][OAc]) on laccase and found that ILs can bind to free enzymes and enzyme–substrate complexes, which in turn inhibits enzyme activity.

Besides acting on enzymes and their interaction, ILs can increase the concentration of substrate in the environment of enzymes, thereby facilitating the reaction. Liu *et al.*[173] investigated the catalytic properties of phenylalanine dehydrogenase in an IL reaction system, where ILs increased the solubility of the hydrophobic substances and increased the concentration of the substrate in the microenvironment of the enzyme, which ultimately led to a 32% increase in activity. In Escudero's study,[168] they also focused on the substrate, increasing its local concentration while decreasing the water activity in the microenvironment of the enzyme, improving the activity and selectivity of the enzyme. In the case of the reaction with CO_2 as the substrate, an increase in the solubility of ILs is undoubtedly more meaningful. Molina-Fernández *et al.*[148] fixed CO_2 with carbonic anhydrase by ILs, and increased the concentration of dissolved CO_2 around the enzyme through the interaction between the ILs and CO_2, thus improving the catalytic efficiency.

In summary, ILs affect the properties of enzymes mainly through stability and activity. ILs can improve their stability mainly by providing a stable environment to protect enzyme molecules from the influence of external factors, while also promoting the activity of enzymes, causing their catalytic reaction rate to increase. The dissolution and polarization of the enzyme molecules by ILs can change the conformation and charge distribution of the enzyme, and thus change the catalytic performance of the enzyme. It should be noted that different ILs may have different effects on different types of enzymes. Factors such as the composition, concentration and environmental conditions of ILs may also affect the stability and activity of enzymes. Therefore, the use of ILs requires the selection of appropriate ILs according to specific conditions and adequate experimental verification.

ILs emerging as cutting-edge candidates in biomedical technology. ILs have emerged as revolutionary tools in the fields of drug delivery, disease diagnosis, and treatment. Their unique properties, such as low volatility, tunable physicochemical characteristics, and biocompatibility, make them cutting-edge candidates as targeted drug delivery systems. In drug delivery, ILs serve as versatile carriers, enhancing the solubility and stability of therapeutic agents, while allowing controlled release profiles. Moreover, ILs play a pivotal role in disease diagnosis by serving as advanced biosensor components, facilitating the more accurate and sensitive detection of pathological conditions. In disease treatment, ILs have demonstrated potential in the treatment various diseases, such as antibacterial, anti-tumor, and antiviral effects. Rogers *et al.*[192] provided a detailed summary on the use of ILs as active pharmaceutical ingredients (API-ILs). API-ILs represent a transformative platform that eliminates solid-state drug problems, while enabling the delivery of various functions, retaining the desirable features of the IL state. By independently and simultaneously tuning the properties of both their anion and cation components, API-ILs offer flexibility in designing new functional pharmaceuticals with altered physicochemical properties such as hygroscopicity, hydrophilicity, liquid range, and stability. This allows the formation of hydrophilic–lipophilic balanced ion pairs for efficient drug delivery and potential synergistic therapeutic actions. The expanding applications of ILs demonstrate their potential to reshape the landscape of pharmaceutical and medical technologies.

ILs in drug delivery

Drug delivery systems serve as a vital platform to efficiently transport drug compounds to their intended targets within the body. These systems offer a range of functions including targeted delivery, controlled release, enhanced bioavailability, protection of drug molecules, and reduced frequency of drug administration. In this case, ILs offer distinct advantages in drug delivery applications primarily due to their versatile chemical nature and unique properties. They can be tailored to solubilize a wide range of drugs, including hydrophobic compounds that are challenging to dissolve in conventional solvents, thereby improving the bioavailability of drugs.[192] ILs

possess adjustable physicochemical characteristics such as viscosity, polarity, and thermal stability, which can be fine-tuned to optimize the drug release kinetics and improve the therapeutic outcomes.[193] ILs also show promise in targeted drug delivery systems through structural modifications such as ligand functionalization and nanoparticle encapsulation, enabling more precise drug delivery to specific sites, while reducing systemic toxicity.[194] However, challenges such as toxicity assessment, scalability of manufacturing processes, and regulatory requirements need to be addressed through further research and development efforts to fully exploit the potential of ILs in clinical settings. Thus, continued exploration and innovation in IL-based drug delivery systems hold significant promise for advancing pharmaceutical therapies with enhanced efficacy and safety profiles. In this section, we provide a detailed introduction on the potential application of ILs in drug delivery systems (Table 3).

ILs as drug solubilizers and transport enhancers

The solubility of a drug is a critical factor affecting its absorption, distribution, and ultimately its effectiveness in the body. Many drugs, particularly those developed recently, face challenges due to their low solubility in water. This low solubility can lead to reduced bioavailability, meaning that the body cannot absorb and use the drug effectively.[195] In this case, the tunable properties of ILs and their capacity to establish specific interactions with other compounds make them promising candidates for enhancing the solubility of drugs. The specific interactions depend on the molecular structure of both the IL and the drug. The ability of ILs to promote the dissolution of poorly soluble drugs often relies on a combination of interactions including H-bonds, π–π stacking, electrostatic interactions, and van der Waals forces.[206] These interactions showcase the potential of ILs to interact with specific functional groups in different drugs, influencing their solubility and, consequently, their bioavailability.[207]

In addition to increasing the solubility of drugs, ILs can also increase their permeability. ILs as permeation enhancers (single agents or combined) in transdermal drug delivery systems have been studied in recent years.[208] Gao *et al.*[197] found that choline-glycolate (CGLY) exhibited the ability to form a gel through H-bonds with polymer chain molecules loaded with Cu^{2+}, effectively replacing the need for toxic chemical crosslinkers. In the treatment process using this gel patch, CGLY facilitated the release of Cu^{2+} through chemodynamic therapy (CDT). This led to the generation of hydroxyl radicals ($^{\bullet}OH$) within the wound, contributing to the eradication of drug-resistant bacteria. Furthermore, the remarkable transdermal performance of CGLY allowed the released Cu^{2+} to stimulate cell migration, expediting the wound healing process. In addition, the gel demonstrated excellent biocompatibility and was proven to be effective in treating skin infection therapy in mice (Fig. 7a).[197]

The interactions between ILs and poorly soluble drugs present an avenue for designing ILs as effective solubilizing agents and drug delivery agents. This strategy shows potential for advancing drug delivery systems and increasing the bioavailability and overcoming challenges related to the low solubility of drugs in the pharmaceutical domain. However, several challenges need to be addressed to fully exploit their potential. The primary concern is the toxicity of ILs, necessitating thorough evaluation of their impact on human health and the environment through comprehensive studies. Stability under physiological conditions is another critical issue, given that ILs must maintain their solubilizing properties in the complex biological environment of the human body. In addition, optimizing the interactions between ILs and various drug molecules is essential for their effective use as solubilizers and

Table 3 ILs applied in drug delivery

Bio-ILs	Effect of Bio-ILs	Advantages	Ref.
Choline lysinate ([Ch][Lys])	Drug solubilizers and permeation enhancers	Improving the solubility and permeation of ferulic acid and puerarin	196
Choline-glycolate (CGLY)	Permeation enhancers	Enhancing the effectiveness and safety of antibacterial hydrogel dressings for wound healing and infection treatment	197
Choline geranic acid ILs (CAGE)	Improving drug bioavailability	Improving solubility of sorafenib, increasing its concentration in the blood, and extending its release time in the body	198
Poly(ionic liquid) nanoparticle	Targeted delivery and controlled release of chemotherapy drugs	Combining targeted ligands, photo-responsive blocks, and pH responsive blocks, with high drug loading capacity	199
Choline-based IL PIL	Drug carrier	Forming amphiphilic systems effectively encapsulated the antibiotic rifampicin, creating single-drug and dual-drug delivery systems	200
Choline-geranate based IL (LATTE)	Drug carrier and ablation agent	Facilitating the internalization of DOX and promoting a microenvironment conducive to immunotherapy	201
$[Bmim]PF_6$	Microwave sensitizer	Enhancing the functionality and efficacy of hollow polydopamine nanoparticles used for combinational cancer therapy	202
1-Butyl-3-methylimidazolium (L)-lactate	Microwave sensitizer	Improved the overall treatment effectiveness	203
Pyridinium-based IL	pH-Responsive agent	Enabling precise control over the release of the anticancer drug methotrexate	204
$[C_8mim]BF_4$	Used to create few-layer IL–$Ti_3C_2T_x$ MXene nanosheets	Enhancing chemical stability and enabling photoacoustic imaging as well as synergistic photothermal/chemotherapy	205

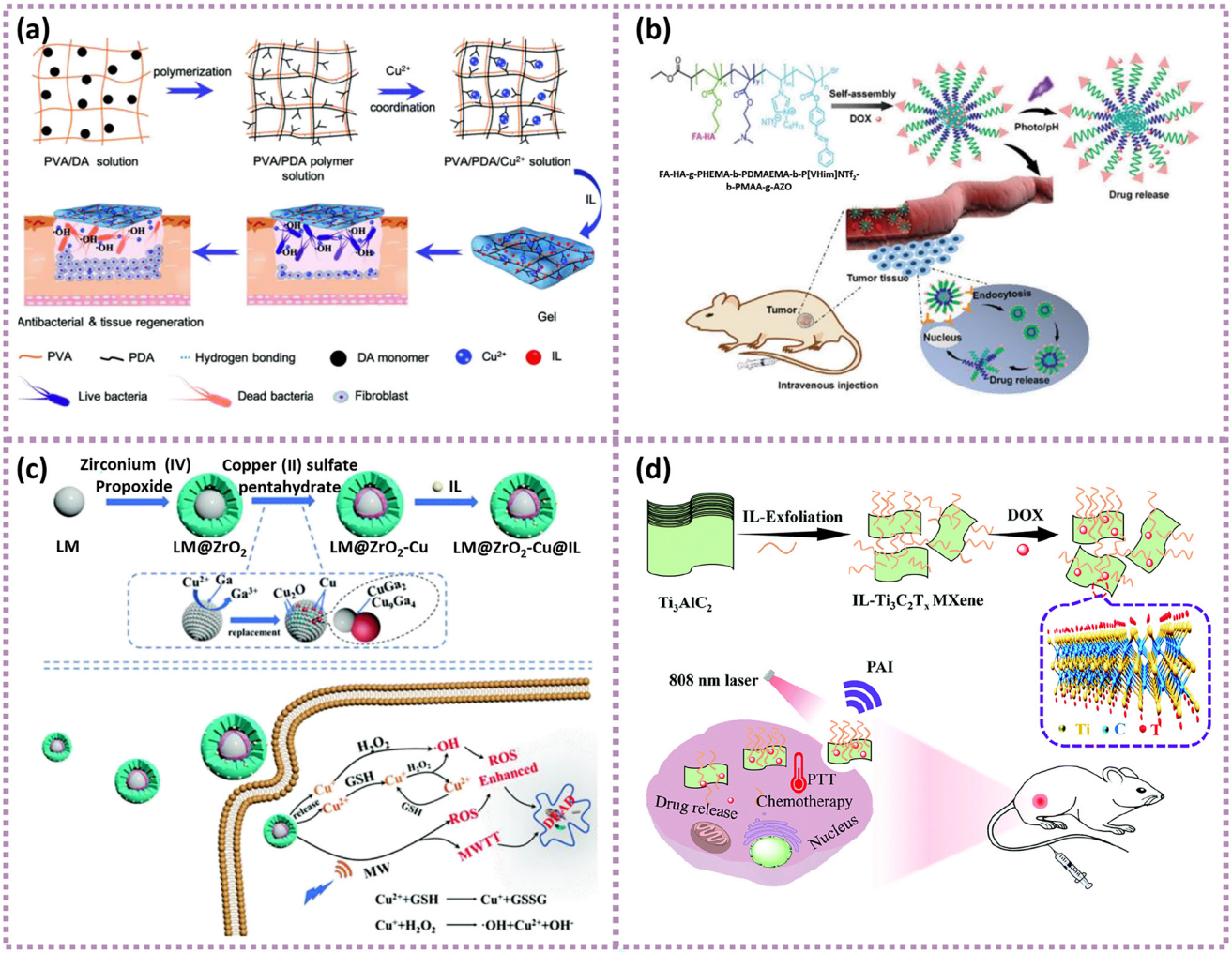

Fig. 7 Application of ILs in drug delivery. (a) IL-copper loaded gel with transdermal delivery function for wound dressings.[197] Reproduced from ref. 197 with permission from The Royal Society of Chemistry, copyright 2022. (b) Release of doxorubicin (DOX) in polymerized IL (PIL-Dox) system, and tumor targeting *in vivo*.[199] Reproduced from ref. 199 with permission from The Royal Society of Chemistry, copyright 2020. (c) Application of ILs in derivative complex drugs. Upper panel: the process of IL-loaded nanocarrier. Lower panel: the IL-nanomaterial system with possible mechanism of therapy.[203] Reproduced from ref. 203 with permission from The Royal Society of Chemistry, copyright 2022. (d) $[C_8mim]BF_4$–$Ti_3C_2T_x$ MXene nanosheets with high chemical stability used for photoacoustic imaging and the synergistic photothermal/chemotherapy of tumors.[205] Reproduced from ref. 205 with permission from The Royal Society of Chemistry, copyright 2022.

transport enhancers. Finally, a deficiency exists in the realm of efficient screening protocols and strategies for the rapid identification of ILs possessing commendable biocompatibility, substantial solubilization capabilities for insoluble drugs, and efficacy in drug delivery. This gap highlights the need for the development of robust screening rules and methodologies in this domain.

Polymerized ILs as drug carriers

The quest for minimizing the side effects and enhancing the therapeutic efficacy of drugs has prompted widespread interest in drug-controlled release systems. Polymerized ILs (PILs) usually have excellent biocompatibility and retain monomer characteristics inherent to ILs. PILs offer several advantages as drug carriers. Firstly, their tunable chemical structure allows the customization of their physicochemical properties, enabling tailored drug delivery systems. Secondly, PILs exhibit high thermal and chemical stability, enhancing their suitability for various drug formulations. Additionally, their ionic nature facilitates efficient drug encapsulation and controlled release, contributing to improved therapeutic efficacy. The biocompatible and biodegradable nature of some PILs further support their potential for biomedical applications.

Lu *et al.*[199] synthesized biocompatible PIL block polymers with a particle size of 80 nm in aqueous solution (Fig. 7b). These drug carriers possessed targeted, pH-responsive, and photo-responsive functions and could effectively load up to 70% DOX. In another study, PILs served as effective drug carriers, as demonstrated by graft copolymers with various IL units.[200] These PILs enabled the creation of both single and

dual-drug delivery systems, utilizing conjugated fusidate (FUS) and encapsulated rifampicin (RIF). The ionic structure of the carriers facilitated ion exchange reactions, resulting in ionic drug–carrier conjugates with self-organizing capabilities.

As we navigate the frontier of pharmaceutical research, the development of PILs stands out as a promising avenue, offering a tailored and controlled approach to realize drug release, which holds the key to optimizing therapeutic outcomes, while mitigating unwanted side effects. However, several challenges must be addressed to fully realize their potential in pharmaceutical applications. The toxicity of PILs and their degradation products remain a major concern, necessitating comprehensive biocompatibility and long-term safety studies. Furthermore, the scalability and economic feasibility of synthesizing PILs on a commercial scale pose practical difficulties, which require innovative solutions to reduce production costs, while maintaining quality. Regulatory hurdles also present significant challenges, given that new drug delivery systems based on PILs must undergo rigorous testing and approval processes, which can be time-consuming and costly. Addressing these challenges through multidisciplinary research and technological advancements is essential for the successful integration of PILs into mainstream drug delivery systems.

ILs in derivative complex drugs

With the development of nanomaterials promoted by recent advances in nano-chemistry, nanoparticles are combined with several functionalities such as imaging, targeting, drug delivery, and therapy, which have been developed *in vivo* to initiate catalytic reactions and modulate biological microenvironments for generating therapeutic effects through various strategies.[209] The important thing is ILs can combine with nanomaterials to form multiple sensitive drug carriers for different irritants, such as microwave, pH- and photo-responsive carriers. ILs combined with nanomaterials have a promising application prospect.

Because of the ionic characteristics and high polarizability of ILs, they are susceptible to microwave radiation,[210] and thus usually used to enhance microwave thermal therapy. Tang and coworkers dedicated their efforts to studying functionalized polydopamine nanoparticles (PDA) loaded with [BMIM][PF_6] as chemotherapeutic drug nanocarriers for combinational therapy. In this report, an IL was the microwave sensitizer.[202] The synthetic IL–PDA–DOX had little damage to normal tissues. Yu *et al.*[203] used 1-butyl-3-methylimidazolium (L)-lactate as a microwave-responsive agent, augmenting microwave thermal therapy. Additionally, the IL improved the overall treatment effectiveness by combining with chemodynamic therapy (CDT) and microwave dynamic therapy (MDT), demonstrating the versatility of ILs in developing multifunctional nanoparticles for advanced cancer treatment strategies (Fig. 7c).

By selecting the appropriate combinations of cations and anions, the structure and properties of ILs can be refined to contain pH sensitive groups and strong photo-sensitive groups. The use of a pyridinium-based IL facilitated the synthesis of pH-responsive cationic silica nanoparticles, enabling precise control of the release of the anticancer drug methotrexate.[204] This pH-triggered release mechanism enhanced the therapeutic efficacy of the drug, while maintaining low cytotoxicity of the carrier nanoparticles. [C_8mim]BF_4 enabled the exfoliation of the MAX phase, resulting in nanosheets with high chemical stability and efficient drug delivery capabilities.[205] These [C_8mim]BF_4–$Ti_3C_2T_x$ MXene nanosheets, when loaded with DOX, exhibited pH- and photo-responsive properties, allowing controlled drug release in the acidic tumor microenvironment and under laser irradiation (Fig. 7d).[205]

The application of nanomaterials is developing rapidly in biomedicine and it has new and unknown properties in combination with diverse ILs, greatly broadening the role and methods of ILs in biomedicine. Also, it provides a new idea for the use of nanomaterials and ILs as new pharmaceutical preparations to treat diseases. However, ILs modifying the surface of nanomaterials may limit the drug loading. Therefore, the surface modification and drug activity should be balanced.

ILs in disease diagnosis

A variety of chemicals such as proteins, glucose, neurotransmitters and others work diligently and regularly to maintain the normal activities in the body. However, when their levels change abnormally, it is likely that there is an abnormality or even a disease, either physically or mentally. Nowadays, various diseases significantly impact human health, emphasizing the importance of early diagnosis, prevention, and treatment. In this case, ILs can play important roles in addressing these needs (Table 4).

ILs in the cancer diagnosis

Cancer is notorious for its suffering, morbidity, and mortality. Thus, it is crucial to diagnose it as early as possible to improve the survival rate of patient,[215] which has attracted attention from many researchers. Zha *et al.*[211] devised a biosensor based on photoelectrochemical and electrochemical properties for analyzing circulating tumor DNA, which was specifically applied for the diagnosis of triple-negative breast cancer (Fig. 8a). They successfully engineered two-dimensional Nd-MOF nanosheets that were functionalized with an IL. Under carefully designed and optimized conditions, the linear range of this sensor extended from 1.0 fmol L^{-1} to 10 nmol L^{-1} for the photoelectrochemical model and from 1.0 fmol L^{-1} to 1.0 nmol L^{-1} for the electrochemical model when measuring the logarithm of circulating tumor DNA concentration. With remarkable accuracy in determining circulating tumor DNA, this feature makes this biosensor promising for the examination of various DNAs, effectively preventing false-negative or false-positive outcomes and expanding its potential applications in the early diagnosis of a wide array of diseases.[211]

Alpha-fetoprotein serves as a widely employed tumor marker. Recognizing its pivotal role in the early diagnosis and its high reliability, Liu *et al.*[212] introduced an innovative mono-

Table 4 ILs applied in disease diagnosis

Disease	Analytes	IL type	Linear range	Ref.
Triple-negative breast cancer	Circulating tumor DNA	$BDBDBIm(Br)_2$	1.0 fmol L^{-1} to 10 nmol L^{-1}	211
Primary hepatoma	Alpha-fetoprotein	Poly guanidinium IL	0.1 to 1000 μg L^{-1}	212
Prostate cancer	Prostate-specific antigen	Tetrabutylphosphonium cation and GB-derived anions	2.5 and 10 ng mL^{-1}	213
Parkinson's disease	Neurotransmitters	Magnetic ILs	0.23–885 arginine 0.38–2600 choline 0.74–1080 dopamine 0.60–1200 epinephrine 0.67–3060 ethanolamine 0.68–3000 γ-aminobutyric acid 0.40–1000 glutamate 54–5400 glutamine 0.20–1000 ornithine 0.35–3360 phenylethylamine 0.30–1180 serine 0.87–1280 threonine 0.70–880 tryptamine 4.82–2000 tryptophan 1.57–1220 tyramine 4.86–3750 tyrosine 1.00–580 3-hydroxyanthranilic acid 0.25–1140 5-methoxytryptamine 0.40–1000 3,4-dihydroxyphenylacetate 0.40–1080 5-hydroxyindoleacetic acid	214

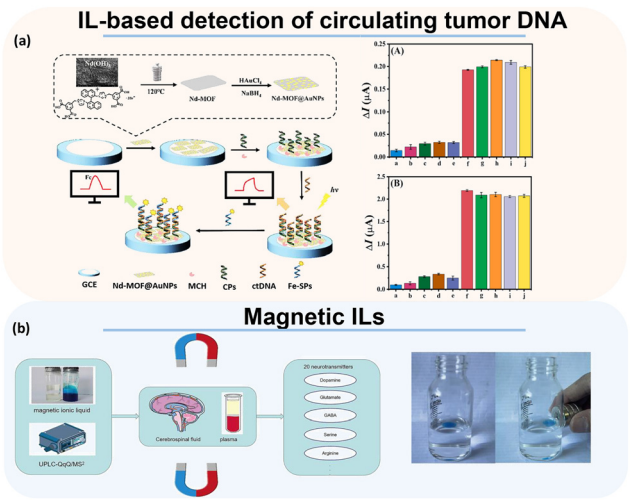

Fig. 8 (a) Schematic of IL-based detection of circulating tumor DNA.[211] Reproduced from ref. 211 with permission from Elsevier, copyright 2023. (b) Magnetic ILs for the diagnosis of Parkinson's disease.[214] Reproduced from ref. 214 with permission from Elsevier, copyright 2023.

lithic material based on a polyguanidinium IL to sensitively detect the alpha-fetoprotein level.[212] This method displayed a linear range of 0.1 to 1000 μg L^{-1}, with a detection limit of 0.05 μg L^{-1}. Notably, this approach successfully determined alpha-fetoprotein in human serum, which is mainly ascribed to its efficacy of exceptional separation and enrichment effects by the polyguanidinium IL material on the targets.[212] Existing techniques for quantifying the prostate-specific antigen (PSA) in human fluid samples require extensive sample handling and involve costly immunoassays. Despite being less frequently utilized in diagnostic procedures, PSA is also present in human urine. Thus, to address these challenges, Pereira *et al.*[213] innovatively constructed ionic-liquid-based aqueous biphasic systems. This approach streamlined the pre-treatment of human urine, providing a more efficient means for quantifying PSA in a non-invasive matrix. Through meticulous design, the IL-based system exhibited the capability to concurrently extract and concentrate PSA, achieving concentrations up to 250-fold higher in the IL-rich phase.[213] This advancement lays the groundwork for expedited and cost-effective equipment utilization in the quantification of PSA, offering promising prospects for the diagnosis of future cases of differential prostate cancer.

ILs in other disease diagnosis

Neurotransmitters are closely linked to neuronal survival, growth, and differentiation, and thus abnormalities in their function indicate underlying diseases. For instance, significant fluctuations in neurotransmission within the basal ganglia have been observed to profoundly influence the pathophysiology of Parkinson's disease.[216] Ding *et al.*[214] employed a magnetic IL-based liquid–liquid microextraction technique in conjunction with a precise, rapid and sensitive ultra-performance liquid chromatography coupled with triple-quadrupole tandem mass spectrometry analytical method to simultaneously determine neurotransmitters in bio-samples

(Fig. 8b). The researchers adopted two types of magnetic ILs, namely $[P_{6,6,6,14}]_3[GdCl_6]$ and $[P_{6,6,6,14}]_2[CoCl_4]$, and ultimately selected $[P_{6,6,6,14}]_2[CoCl_4]$ as the extraction solvent because of its paramagnetic behavior, superior extraction efficiency, and visual recognition benefits. Notably, the application of an external magnetic field facilitated its easy magnetic separation, eliminating the need for centrifugation, given that the magnetic ILs efficiently extracted the analytes from the matrix. Following the optimization of various parameters, their method successfully achieved the simultaneous extraction and detection of 20 neurotransmitters in human plasma and cerebrospinal fluid samples, demonstrating broad clinical applications in the field of diagnosis.[214]

ILs in diseases therapy

Medication or treatment should be administered as early as possible during the early to middle stages of an illness in patients. In this case, ILs consist solely of anion and cation combinations, offering a wide array of combinations. Among them, many are favorable for the treatment of diseases.

ILs in antibacterial therapy

The poor treatment of wounds in patients is exacerbated by the overuse of antibiotics and the emergence of bacteria resistant to antibacterial agents. Accordingly, ILs offer a promising avenue for addressing this challenge. They can not only extract and transport antibacterial substances efficiently due to their excellent solubility and biocompatibility but also by designing new substances such as ILs, they can become a favorable strategy for effective treatment.[217–219]

Bonyadi *et al.*[220] investigated the isolation of 60 *E. faecalis* strains from oral infections and assessed the presence, frequency and expression of genes using real-time PCR in conjunction with ILs. The results of minimum and sub-minimum inhibitory concentrations demonstrated the effect of the ILs (containing methionine base) at concentrations of 125 and 225 μg mL^{-1}, respectively. Remarkably, the amino-acid-based ILs were observed to reduce biofilm production at sub-minimum inhibitory concentrations. The genetic variability among the *E. faecalis* strains was identified, and the combined treatment of IL with conventional antimicrobial drugs exhibited excellent antibacterial efficiency against *Enterococcus* species. The application of IL at a minimum dose showed promise as a desirable alternative to single-drug treatment of *Enterococcus* infections.[220] In a related study, Zhang *et al.*[221] used tetrakis(hydroxymethyl)phosphonium chloride, a phosphonium-based IL with numerous hydroxyl groups, as a biocide to modify a PEI/TMC membrane. This IL enhanced the antibacterial properties, permeability, and various surface characteristics of the original membranes, including morphology, zeta potential, hydrophilicity, and roughness.[221] Shi *et al.*[222] synthesized a series of aggregation-induced emission (AIE)-based imidazolium ILs, with bactericidal ability, low cytotoxicity and hemolysis. These ILs demonstrated the capacity to selectively capture fluorescence images of dead bacteria in blood cells, while effectively eliminating the bacteria. In addition, the fluorescence intensity increased with an enhancement in the bacteria concentration. Thus, AIE-based ILs show great potential as probes for diagnosis and anti-bacterial treatment simultaneously.

ILs in anticancer therapy

Chemotherapy is used as the most common cancer treatment modality due to its rapid and targeted action.[223] Unfortunately, the compounds used in chemotherapy often exhibit toxicity to normal cells. In addition, solubility poses another limitation in the use of chemotherapy agents. Consequently, the quest for new chemotherapeutic molecules, as well as targeted therapies, is a burgeoning area of research. ILs have emerged as promising candidates possessing anticancer activity against a variety of tumor cells.

Ali *et al.*[224] engineered hybrids by integrating imidazolium ILs and thiohydantoin motifs together with their Mn/Fe(III) complexes for application in anticancer therapy. These novel hybrids showed heightened effectiveness and selectivity in inhibiting the proliferation of MCF-7 cells compared to HepG2 cells.[224] In a study led by Sangeeta *et al.*, derivatives of a 1,3-benzodioxole-tagged lidocaine-based IL were designed and synthesized. The binding affinities for [Pip-Lid]OAc and [Pip-Lid]OTf were calculated to be −384.47 kJ mol^{-1} and −355.74 kJ mol^{-1}, respectively. The properties of these ILs, including blood–brain barrier permeability and drug-likeliness, underscored the potential efficacy of the compound for treating skin cancer. *In silico* work elucidated that the primary interaction forces involved hydrophobic and weak electrostatic interactions, together with hydrogen bonds.[225] This multifaceted approach provided valuable insights into the molecular dynamics of these compounds, offering a foundation for further research in the field of cancer treatment.

Conclusion and perspectives

ILs, with their unique physicochemical properties, are promising in new energy (battery energy storage, hydrogen energy, and solar energy), electronic information chemicals (two-dimensional materials and photoresist), biotechnologies (biocatalysis and biomedicine), and other emerging fields. In this review, we summarized the development history of the structure (four generations) and nature (from Z-bonds to quasi-liquids and clusters) of ILs. Considering the structural and theoretical findings, we then explored four cutting-edge applications of ILs in terms of their potential functions. The current state of the art in the emerging fields has proven the feasibility of the advantageous applications for ILs. Nevertheless, considerable challenges still need to be addressed in future work to advance the development of green and low-carbon transformations. Thus, to address the various issues associated with the applications of ILs, there is a need to deepen the scientific understanding of their nature and function, as well as to strengthen multidisciplinary collaborations.

(1) ILs are promising electrolyte candidates for rechargeable metal batteries, where their rich anions can enable the formation of an inorganic-rich SEI, thus stabilizing the metal plating. However, function mechanism of ILs in batteries still needs to be clarified, especially in terms of the solvation structure of the cations, the trade-off between rich anions and reduced metal ion transference number, and the cation/anion interactions in the electric field, which are all vital for future applications in this area. In these considerations, the combination of *in situ* or *operando* equipment and multi-scale simulation should be great tool in the relevant study.

(2) To date, Nafion® is the most researched and used proton exchange membrane. However, due to its obvious drawbacks, such as high cost and poor high temperature and anhydrous condition performance, the addition of fillers to Nafion® matrices is commonly performed but does not guarantee an improvement in all membrane properties. The use of inorganic fillers improves the thermo-mechanical properties and oxidative stability of the membranes, while reducing their proton conductivity. Alternatively, the use of IL fillers can enhance the conductivity, especially at high temperatures. However, it decreases the thermo-mechanical stability of the membrane. Therefore, the use of both types of above-mentioned fillers seems to be a promising approach for obtaining high-yield Nafion®-based composite membranes.

(3) In PSCs, we firmly believe that the incorporation of ILs holds potential to inhibit ion migration, offering a viable avenue to obstruct the degradation of the perovskite absorbers, thereby advancing the prospect of commercializing PSCs in the future. Nevertheless, unresolved issues exist, which are outlined as follows. Besides the state-of-the-art studies, the comprehensive interaction mechanism between perovskite and ILs for preferred crystal orientation remains elusive. Therefore, a deep mechanistic study is urgently needed to determine the role played by ILs in governing the preferred crystal orientation for optimizing the fabrication process of high-quality perovskite films. The functional role of ILs within PSCs depends on their spatial distribution, yet the factors governing their disparate localization remain unclear. Clarifying this mechanism holds promise for tailored IL design or process optimization to regulate their position, thereby facilitating targeted functional outcomes.

(4) Task-specific ILs can be used as exfoliation agents, liquid substances, and ILGs to obtain 2D electronic materials, wafer-sized single crystals and semiconductor junctions, which is of great significance for the development of high-end electronic materials. As the most important material in the lithography process, the photoresist determines the reliability of lithographic patterns. With the advancement of Moore's law and the increasing chip integration, the research on the corresponding high-resolution photoresists has received more extensive attention in the fields of lithography and nanomaterials. The sensitivity, etch resistance and roughness control of photoresists encounter unprecedented challenges in the processing of structures corresponding to the 20 nm technology node and below, as well as the requirements of industrialized and efficient production, in addition to the significant increase in cost due to multiple patterning techniques, and the difficulty in controlling the nesting accuracy between masks. DSA lithography, in combination with traditional top-down EUV lithography, deep UV lithography, and UV lithography, can increase the existing graphic resolution, repair graphic defects, and improve the feature size uniformity. With continuous process optimization, DSA lithography has made great strides in improving the resolution, reducing the defect density, optimizing the feature size uniformity and reducing the line edge roughness and will be widely used in microelectronic manufacturing, such as FinFETs, memories, BPMs and photonic devices.

(5) In terms of biocatalysis, a better understanding of the interaction mechanism between ILs and enzymes at the atomic level will help select the ILs acting in the enzyme system. This requires some cross-disciplinary research, such as computer modeling and simulation. Relevant modifications can be made to enzymes to develop enzymes more adapted to the IL environment through bioinformatics and protein engineering, which will help ILs better promote the efficiency of enzyme reactions. Furthermore, the possibility of exploring the recyclability and scaled-up production of ILs requires us to find better separation and purification methods, which are still lacking in terms of greenness and economy in the current methods. The research and optimization of IL bioreaction systems in the above-mentioned aspects can open up broader prospects for the development in green biocatalysis.

(6) Additionally, ILs have emerged as game-changers in the fields of drug delivery, disease diagnosis, and treatment, presenting a wide range of innovative applications. The ability of ILs to encapsulate and protect sensitive bioactive compounds during transit to the target sites makes them invaluable in developing advanced drug delivery systems. Furthermore, ILs enhance the sensitivity and selectivity of diagnostic assays for biomolecules, enabling the early detection of diseases. Besides, the continuous evolution of ILs as active pharmaceutical components holds potential to revolutionize drug discovery and propel the biopharmaceutical field towards new frontiers of innovation.

(7) The toxicity and environmental impact of ILs are critical concerns that need thorough evaluation. Life cycle analysis (LCA) is an essential tool in this regard, providing a comprehensive assessment of the environmental aspects and potential impacts associated with ILs from the production to disposal. The toxicity of ILs can widely vary depending on their chemical structure. Although some ILs are designed to be environmentally benign, others can be harmful to the aquatic and terrestrial ecosystems. For instance, certain cation–anion combinations in ILs can lead to bioaccumulation and adverse effects on organisms. Thus, this variability necessitates the careful selection and design of ILs for specific applications, ensuring they are both effective and environmentally friendly. LCA examines the environmental impacts of ILs throughout their entire life cycle, from raw material extraction, synthesis, and use, to end-of-life disposal or recycling. This holistic

approach helps identify stages, where improvements can be made to minimize their environmental footprint. For example, the synthesis of ILs often involves energy-intensive processes and the use of hazardous chemicals, which can be optimized to reduce emissions and waste. Additionally, the end-of-life phase is crucial, given that the improper disposal of ILs can lead to the contamination of water bodies and soil.

(8) It should be noted that ILs have been criticised for their cost in large-scale applications. Therefore, improving the economics of ILs will become an urgent problem for industry and academia to solve. Presently, two paths are expected to provide ideas to address this issue. Firstly, optimizing the preparation process of traditional ILs (the design of the synthesis reactor, the optimization of the purification process, the choice of decolourant, *etc*.) and promoting the industrialisation of new synthesis strategies (such as microwave-assisted synthesis and ultrasound-assisted synthesis) are necessary. In addition, exploring a new generation of cost-effective ILs or IL analogues (such as deep eutectic solvents, DESs) will also be at the forefront of research. Meanwhile, their stability, recyclability, and toxicity should be further investigated before their application.

Data availability

No primary research results, software or code have been included and no new data were generated or analysed as part of this review.

Conflicts of interest

There are no conflicts to declare.

Acknowledgements

This work was supported by the National Key Projects for Fundamental Research and Development of China (grant number 2019YFA0705600), the National Natural Science Foundation of China (grant number 22393960, 22078346), Science Fund for Creative Research Groups of the National Natural Science Foundation of China (grant number 21921005).

References

1 K. Dong, X. Liu, H. Dong, X. Zhang and S. Zhang, *Chem. Rev.*, 2017, **117**, 6636–6695.
2 E. Kianfar and S. Mafi, *Fine Chem. Eng.*, 2020, **2**, 22–31.
3 K. Dong and S. Zhang, *Sci. China: Chem.*, 2021, **51**, 1425–1434.
4 P. Walden, *Bull. Acad. Imp. Sci. St.-Petersbourg*, 1914, **8**, 405–422.
5 F. H. Hurley and T. P. Wier, *J. Electrochem. Soc.*, 1951, **98**, 207.
6 J. Wilkes and M. Zaworotko, *J. Chem. Soc., Chem. Commun.*, 1992, 965–967.
7 M. Demurtas, V. Onnis, P. Zucca, A. Rescigno, J. I. Lachowicz, L. De Villiers Engelbrecht, M. Nieddu, G. Ennas, A. Scano, F. Mocci and F. Cesare Marincola, *ACS Sustainable Chem. Eng.*, 2021, **9**, 2975–2986.
8 A. Benedetto and P. Ballone, *ACS Sustainable Chem. Eng.*, 2016, **4**, 392–412.
9 K. Dong, S. Zhang and J. Wang, *Chem. Commun.*, 2016, **52**, 6744–6764.
10 D. R. MacFarlane, A. L. Chong, M. Forsyth, M. Kar, R. Vijayaraghavan, A. Somers and J. M. Pringle, *Faraday Discuss.*, 2018, **206**, 9–28.
11 C. Wang, Y. Wang, Z. Gan, Y. Lu, C. Qian, F. Huo, H. He and S. Zhang, *Chem. Sci.*, 2021, **12**, 15503–15510.
12 Y. Wang, J. Liu, X. Yuan, M. Wang, Y. Nie, S. Zhang and H. He, *Chem. Eng. J.*, 2023, **455**, 140370.
13 K. Liu, Z. Wang, L. Shi, S. Jungsuttiwong and S. Yuan, *J. Energy Chem.*, 2021, **59**, 320–333.
14 K. Matuszek, S. L. Piper, A. Brzeczek-Szafran, B. Roy, S. Saher, J. M. Pringle and D. R. MacFarlane, *Adv. Mater.*, 2024, **36**, e2313023.
15 A. Ray and B. Saruhan, *Materials*, 2021, **14**, 2942.
16 S. Sheikh and A. Haghpanah Jahromi, *Monatsh. Chem.*, 2024, **155**, 383–399.
17 T. Zhou, C. Gui, L. Sun, Y. Hu, H. Lyu, Z. Wang, Z. Song and G. Yu, *Chem. Rev.*, 2023, **123**, 12170–12253.
18 W. Zhou, M. Zhang, X. Kong, W. Huang and Q. Zhang, *Adv. Sci.*, 2021, **8**, 2004490.
19 Y. Lu, S. K. Das, S. S. Moganty and L. A. Archer, *Adv. Mater.*, 2012, **24**, 4430–4435.
20 A. Basile, A. I. Bhatt and A. P. O'Mullane, *Nat. Commun.*, 2016, **7**, 11794.
21 X. Wang, M. Salari, D. Jiang, J. Chapman Varela, B. Anasori, D. J. Wesolowski, S. Dai, M. W. Grinstaff and Y. Gogotsi, *Nat. Rev. Mater.*, 2020, **5**, 787–808.
22 X. Liu, A. Mariani, H. Adenusi and S. Passerini, *Angew. Chem., Int. Ed.*, 2023, **62**, e202219318.
23 X. Ma, J. Yu, Y. Hu, J. Texter and F. Yan, *Ind. Chem. Mater.*, 2023, **1**, 39–59.
24 X. Liu, A. Mariani, T. Diemant, X. Dong, P. H. Su and S. Passerini, *Angew. Chem., Int. Ed.*, 2023, e202305840.
25 X. Liu, A. Mariani, T. Diemant, M. E. Di Pietro, X. Dong, A. Mele and S. Passerini, *Adv. Mater.*, 2023, **36**, 2309062.
26 K. Sirengo, A. Babu, B. Brennan and S. C. Pillai, *J. Energy Chem.*, 2023, **81**, 321–338.
27 H. Sun, G. Zhu, X. Xu, M. Liao, Y. Li, M. Angell, M. Gu, Y. Zhu, W. Hung, J. Li, Y. Kuang, Y. Meng, M. Lin, H. Peng and H. Dai, *Nat. Commun.*, 2019, **10**, 3302.
28 M. Fiore, S. Wheeler, K. Hurlbutt, I. Capone, J. Fawdon, R. Ruffo and M. Pasta, *Chem. Mater.*, 2020, **32**, 7653–7661.
29 X. Gao, A. Mariani, S. Jeong, X. Liu, X. Dou, M. Ding, A. Moretti and S. Passerini, *J. Power Sources*, 2019, **423**, 52–59.
30 J. Qin, Q. Lan, N. Liu, F. Men, X. Wang, Z. Song and H. Zhan, *iScience*, 2019, **15**, 16–27.

31 T. Fromling, M. Kunze, M. Schonhoff, J. Sundermeyer and B. Roling, *J. Phys. Chem. B*, 2008, **112**, 12985–12990.
32 X. Liu, T. Diemant, A. Mariani, X. Dong, M. E. Di Pietro, A. Mele and S. Passerini, *Adv. Mater.*, 2022, **34**, e2207155.
33 K. Yamaguchi, Y. Domi, H. Usui, M. Shimizu, S. Morishita, S. Yodoya, T. Sakata and H. Sakaguchi, *J. Electrochem. Soc.*, 2019, **166**, A268–A276.
34 X. Liu, Y. Ren, L. Zhang and S. Zhang, *Front. Chem.*, 2019, **7**, 421.
35 Y. Cheng, L. Zhang, S. Xu, H. Zhang, B. Ren, T. Li and S. Zhang, *J. Mater. Chem. A*, 2018, **6**, 18479–18487.
36 Z. Huang, J. Lai, S. Liao, Z. Yu, Y. Chen, W. Yu, H. Gong, X. Gao, Y. Yang, J. Qin, Y. Cui and Z. Bao, *Nat. Energy*, 2023, **8**, 577–585.
37 Z. Huang, J. Lai, X. Kong, I. Rajkovic, X. Xiao, H. Celik, H. Yan, H. Gong, P. E. Rudnicki, Y. Lin, Y. Ye, Y. Li, Y. Chen, X. Gao, Y. Jiang, S. Choudhury, J. Qin, J. B. H. Tok, Y. Cui and Z. Bao, *Matter*, 2023, **6**, 445–459.
38 N. Sanchez-Ramirez, B. D. Assresahegn, R. M. Torresi and D. Bélanger, *Energy Storage Mater.*, 2020, **25**, 477–486.
39 D. T. Rogstad, M. A. Einarsrud and A. M. Svensson, *J. Electrochem. Soc.*, 2021, **168**, 110506.
40 N. Sánchez-Ramírez, I. E. Monje, D. Bélanger, P. H. C. Camargo and R. M. Torresi, *Electrochim. Acta*, 2023, **439**, 141680.
41 Y. Zhang, J. Huang, H. Liu, W. Kou, Y. Dai, W. Dang, W. Wu, J. Wang, Y. Fu and Z. Jiang, *Adv. Energy Mater.*, 2023, **13**, 2300156.
42 S. Xu, Y. Cheng, L. Zhang, K. Zhang, F. Huo, X. Zhang and S. Zhang, *Nano Energy*, 2018, **51**, 113–121.
43 A. Kondori, M. Esmaeilirad, A. M. Harzandi, R. Amine, M. T. Saray, L. Yu, T. Liu, J. Wen, N. Shan, H. Wang, A. T. Ngo, P. C. Redfern, C. S. Johnson, K. Amine, R. Shahbazian-Yassar, L. A. Curtiss and M. Asadi, *Science*, 2023, **379**, 499–505.
44 W. Wu, A. Wang, Q. Zhan, Z. Hu, W. Tang, L. Zhang and J. Luo, *Small*, 2023, **19**, e2301737.
45 D. Stepien, B. Wolff, T. Diemant, G. T. Kim, F. Hausen, D. Bresser and S. Passerini, *ACS Appl. Mater. Interfaces*, 2023, **15**, 25462–25472.
46 X. Wang, F. Chen, G. M. A. Girard, H. Zhu, D. R. MacFarlane, D. Mecerreyes, M. Armand, P. C. Howlett and M. Forsyth, *Joule*, 2019, **3**, 2687–2702.
47 K. Pan, L. Zhang, W. Qian, X. Wu, K. Dong, H. Zhang and S. Zhang, *Adv. Mater.*, 2020, **32**, e2000399.
48 Q. Zhang, K. Pan, M. Jia, X. Zhang, L. Zhang, H. Zhang and S. Zhang, *Electrochim. Acta*, 2021, **368**, 137593.
49 Y. Liu, J. Cui, H. Wang, K. Wang, Y. Tian, X. Xue, Y. Qiao, X. Ji and S. Zhang, *Green Chem.*, 2023, **25**, 4981–4994.
50 A. Nasri, B. Jaleh, E. Shabanlou, M. Nasrollahzadeh, H. Ali Khonakdar and B. Kruppke, *J. Mol. Liq.*, 2022, **365**, 120142.
51 T. Le, P. Sharma, B. J. Bora, V. D. Tran, T. H. Truong, H. C. Le and P. Q. P. Nguyen, *Int. J. Hydrogen Energy*, 2024, **54**, 791–816.
52 M. S. Tutgun, D. Sinirlioglu, S. U. Celik and A. Bozkurt, *J. Polym. Res.*, 2015, **22**, 101198.
53 D. J. Kim, M. J. Jo and S. Y. Nam, *J. Ind. Eng. Chem.*, 2015, **21**, 36–52.
54 D. Sinirlioglu, S. Ü. Çelik, A. E. Muftuoglu and A. Bozkurt, *Polym. Eng. Sci.*, 2015, **55**, 260–269.
55 N. H. Kim, A. K. Mishra, D. Y. Kim and J. H. Lee, *Chem. Eng. J.*, 2015, **272**, 119–127.
56 A. K. Mishra, S. Bose, T. Kuila, N. H. Kim and J. H. Lee, *Prog. Polym. Sci.*, 2012, **37**, 842–869.
57 J. A. Mader and B. C. Benicewicz, *Fuel Cells*, 2011, **11**, 222–237.
58 S. J. Peighambardoust, S. Rowshanzamir and M. Amjadi, *Int. J. Hydrogen Energy*, 2010, **35**, 9349–9384.
59 E. B. Cho, D. X. Luu and D. Kim, *J. Membr. Sci.*, 2010, **351**, 58–64.
60 N. Awang, A. F. Ismail, J. Jaafar, T. Matsuura, H. Junoh, M. H. D. Othman and M. A. Rahman, *React. Funct. Polym.*, 2015, **86**, 248–258.
61 L. Zanchet, L. G. da Trindade, W. Bariviera, K. M. Nobre Borba, R. D. M. Santos, V. A. Paganin, C. P. de Oliveira, E. A. Ticianelli, E. M. A. Martini and M. O. de Souza, *J. Mater. Sci.*, 2020, **55**, 6928–6941.
62 K. Fatyeyeva, S. Rogalsky, S. Makhno, O. Tarasyuk, J. A. Soto Puente and S. Marais, *Membranes*, 2020, **10**, 82.
63 X. Wang, M. Jin, Y. Li and L. Zhao, *Electrochim. Acta*, 2017, **257**, 290–300.
64 S. Maity, S. Singha and T. Jana, *Polymer*, 2015, **66**, 76–85.
65 S. Liu, L. Zhou, P. Wang, F. Zhang, S. Yu, Z. Shao and B. Yi, *ACS Appl. Mater. Interfaces*, 2014, **6**, 3195–3200.
66 D. Langevin, Q. T. Nguyen, S. Marais, S. Karademir, J. Y. Sanchez, C. Iojoiu, M. Martinez, R. Mercier, P. Judeinstein and C. Chappey, *J. Phys. Chem. C*, 2013, **117**, 15552–15561.
67 T. K. Maiti, P. Dixit, J. Singh, N. Talapatra, M. Ray and S. Chattopadhyay, *Int. J. Hydrogen Energy*, 2023, **48**, 1482–1500.
68 Y. Li, J. Hu, H. Li and L. Chen, *J. Electrochem. Soc.*, 2022, **169**, 024505.
69 K. S. Khoo, W. Y. Chia, K. Wang, C. K. Chang, H. Y. Leong, M. N. B. Maaris and P. L. Show, *Sci. Total Environ.*, 2021, **793**, 148705.
70 E. Qu, G. Cheng, M. Xiao, D. Han, S. Huang, Z. Huang, W. Liu, S. Wang and Y. Meng, *J. Mater. Chem. A*, 2023, **11**, 12885–12895.
71 A. Shabanikia, M. Javanbakht, H. S. Amoli, K. Hooshyari and M. Enhessari, *Ionics*, 2015, **21**, 2227–2236.
72 D. Yu, Y. Cui, S. Wang, X. Wang, Z. Yong, H. Sun, X. Wang, C. Li, F. Pan and Z. Wang, *Int. J. Hydrogen Energy*, 2023, **48**, 9023–9036.
73 Q. Liu, C. Xiong, H. Shi, L. Liu, X. Wang, X. Fu, R. Zhang, S. Hu, X. Bao, X. Li, F. Zhao and C. Xu, *J. Membr. Sci.*, 2023, **668**, 121192.
74 G. Wei, Y. Liu, A. Wu, Y. Min, Z. Liao, R. Zhu, Y. Liang and L. Wang, *Mater. Today Chem.*, 2023, **27**, 101276.

75 P. Wang, J. Lin, Y. Wu and L. Wang, *J. Power Sources*, 2023, **560**, 232665.
76 X. Wang, D. Wang, S. Wang, J. Li, G. Liu, Y. Cui, D. Liang, X. Wang, Z. Yong and Z. Wang, *ACS Appl. Energy Mater.*, 2022, **5**, 2553–2563.
77 S. M. Park, M. Wei, J. Xu, H. R. Atapattu, F. T. Eickemeyer, K. Darabi, L. Grater, Y. Yang, C. Liu, S. Teale, B. Chen, H. Chen, T. Wang, L. Zeng, A. Maxwell, Z. Wang, K. R. Rao, Z. Cai, S. M. Zakeeruddin, J. T. Pham, C. M. Risko, A. Amassian, M. G. Kanatzidis, K. R. Graham, M. Grätzel and E. H. Sargent, *Science*, 2023, **381**, 209–215.
78 J. Park, J. Kim, H. Yun, M. J. Paik, E. Noh, H. J. Mun, M. G. Kim, T. J. Shin and S. I. Seok, *Nature*, 2023, **616**, 724–730.
79 Y. Lin, N. Sakai, P. Da, J. Wu, H. C. Sansom, A. J. Ramadan, S. Mahesh, J. Liu, R. D. J. Oliver, J. Lim, L. Aspitarte, K. Sharma, P. K. Madhu, A. B. Morales-Vilches, P. K. Nayak, S. Bai, F. Gao, C. R. M. Grovenor, M. B. Johnston, J. G. Labram, J. R. Durrant, J. M. Ball, B. Wenger, B. Stannowski and H. J. Snaith, *Science*, 2020, **369**, 96–102.
80 J. Luo, F. Lin, J. Yuan, Z. Wan and C. Jia, *ACS Mater. Lett.*, 2022, **4**, 1684–1715.
81 J. Yang, J. Hu, W. Zhang, H. Han, Y. Chen and Y. Hu, *J. Energy Chem.*, 2023, **77**, 157–171.
82 R. Xia, X. Gao, Y. Zhang, N. Drigo, V. I. E. Queloz, F. F. Tirani, R. Scopelliti, Z. Huang, X. Fang, S. Kinge, Z. Fei, C. Roldán-Carmona, M. K. Nazeeruddin and P. J. Dyson, *Adv. Mater.*, 2020, **32**, 2003801.
83 S. Bai, P. Da, C. Li, Z. Wang, Z. Yuan, F. Fu, M. Kawecki, X. Liu, N. Sakai, J. T.-W. Wang, S. Huettner, S. Buecheler, M. Fahlman, F. Gao and H. J. Snaith, *Nature*, 2019, **571**, 245–250.
84 S. Ghosh and T. Singh, *Nano Energy*, 2019, **63**, 103828.
85 X. Zhou, Y. Wang, C. Li and T. Wu, *Chem. Eng. J.*, 2019, **372**, 46–52.
86 H. Wu, Z. Li, F. Zhang, C. Kang and Y. Li, *Adv. Mater. Interfaces*, 2022, **9**, 2201292.
87 J. Seo, T. Matsui, J. Luo, J. Correa-Baena, F. Giordano, M. Saliba, K. Schenk, A. Ummadisingu, K. Domanski, M. Hadadian, A. Hagfeldt, S. M. Zakeeruddin, U. Steiner, M. Grätzel and A. Abate, *Adv. Energy Mater.*, 2016, **6**, 1600767.
88 Z. Chen, L. Wang, J. Fang, A. Saeed, K. Wang and Q. Miao, *ACS Appl. Energy Mater.*, 2023, **6**, 8489–8494.
89 P. Hu, S. Huang, M. Guo, Y. Li and M. Wei, *ChemSusChem*, 2022, **15**, e202200819.
90 F. Wang, P. Wai-Keung Fong, Z. Ren, H. Xia, K. Zhou, K. Wang, J. Zhu, X. Huang, X. Liu, H. Wang, Y. Shi, H. Lin, Q. Zhu, G. Li and H. Hu, *J. Energy Chem.*, 2022, **73**, 599–606.
91 S. Akin, E. Akman and S. Sonmezoglu, *Adv. Funct. Mater.*, 2020, **30**, 2002964.
92 Y. Guo, K. Shoyama, W. Sato, Y. Matsuo, K. Inoue, K. Harano, C. Liu, H. Tanaka and E. Nakamura, *J. Am. Chem. Soc.*, 2015, **137**, 15907–15914.
93 L. Chao, T. Niu, H. Gu, Y. Yang, Q. Wei, Y. Xia, W. Hui, S. Zuo, Z. Zhu, C. Pei, X. Li, J. Zhang, J. Fang, G. Xing, H. Li, X. Huang, X. Gao, C. Ran, L. Song, L. Fu, Y. Chen and W. Huang, *Research*, 2020, 2616345.
94 W. Hui, L. Chao, H. Lu, F. Xia, Q. Wei, Z. Su, T. Niu, L. Tao, B. Du, D. Li, Y. Wang, H. Dong, S. Zuo, B. Li, W. Shi, X. Ran, P. Li, H. Zhang, Z. Wu, C. Ran, L. Song, G. Xing, X. Gao, J. Zhang, Y. Xia, Y. Chen and W. Huang, *Science*, 2021, **371**, 1359–1364.
95 L. Gu, C. Ran, L. Chao, Y. Bao, W. Hui, Y. Wang, Y. Chen, X. Gao and L. Song, *ACS Appl. Mater. Interfaces*, 2022, 35077147.
96 F. Wang, Y. Han, D. Duan, C. Ge, H. Hu and G. Li, *Energy Rev.*, 2022, **1**, 100010.
97 F. Wang, K. Zhou, X. Liang, X. Zhou, D. Duan, C. Ge, X. Zhang, Y. Shi, H. Lin, Q. Zhu, L. Li, H. Hu and H. Zhang, *Small Methods*, 2023, **8**, 2300210.
98 W. Zhang, X. Liu, B. He, Z. Gong, J. Zhu, Y. Ding, H. Chen and Q. Tang, *ACS Appl. Mater. Interfaces*, 2020, **12**, 4540–4548.
99 X. Huang, H. Guo, K. Wang and X. Liu, *Org. Electron.*, 2017, **41**, 42–48.
100 L. Shi, H. Yuan, X. Sun, X. Li, W. Zhu, J. Wang, L. Duan, Q. Li, Z. Zhou, Z. Huang, X. Ban and D. Zhang, *ACS Appl. Energy Mater.*, 2021, **4**, 10584–10592.
101 D. Gao, L. Yang, X. Ma, X. Shang, C. Wang, M. Li, X. Zhuang, B. Zhang, H. Song, J. Chen and C. Chen, *J. Energy Chem.*, 2022, **69**, 659–666.
102 S. A. Iyengar, S. Bhattacharyya, S. Roy, N. R. R. Glavin, A. K. K. Roy and P. M. M. Ajayan, *ACS Nano*, 2023, **17**, 12955–12970.
103 X. Li, J. Yang, H. Sun, L. Huang, H. Li and J. Shi, *Adv. Mater.*, 2023, 2305115.
104 S. Wang, X. Liu and P. Zhou, *Adv. Mater.*, 2022, **34**, 2106886.
105 C. Lecuyer, *Enterp. Soc.*, 2022, **23**, 133–163.
106 Z. Sun and H. Chang, *ACS Nano*, 2014, **8**, 4133–4156.
107 T. Xing, A. He, Z. Huang, Y. Luo, Y. Zhang, M. Wang, Z. Shi, G. Ke, J. Bai, S. Zhao, F. Chen and W. Xu, *Chem. Eng. J.*, 2023, **474**, 145534.
108 Y. Jiang, Y. Yang, L. Shen, J. Ma, H. Ma and N. Zhu, *Anal. Chem.*, 2022, **94**, 297–311.
109 L. Zhang, J. Dong and F. Ding, *Chem. Rev.*, 2021, **121**, 6321–6372.
110 K. Zhu, C. Wen, A. A. Aljarb, F. Xue, X. Xu, V. Tung, X. Zhang, H. N. Alshareef and M. Lanza, *Nat. Electron.*, 2021, **4**, 775–785.
111 J. Chen, J. Wang, S. Chen, J. Pan, R. Jia, C. Wang, X. Wu, J. Jie and X. Zhang, *Adv. Funct. Mater.*, 2023, **34**, 2308298.
112 J. Wang, Z. Ren, J. Pan, X. Wu, J. Jie, X. Zhang and X. Zhang, *Adv. Mater.*, 2023, **35**, 2309062.
113 X. Yan, Y. Zhao, G. Cao, X. Li, C. Gao, L. Liu, S. Ahmed, F. Altaf, H. Tan, X. Ma, Z. Xie and H. Zhang, *Adv. Sci.*, 2023, **10**, 2203889.
114 R. Biswas, *J. Mol. Liq.*, 2021, **337**, 116592.
115 K. Li, B. He, J. Liu, H. Zhang, R. Zhang, R. Liu, Y. Song and S. Zhang, *Appl. Catal., A*, 2019, **582**, 117106.

116 T. Zhao, J. Guo, T. Li, Z. Wang, M. Peng, F. Zhong, Y. Chen, Y. Yu, T. Xu, R. Xie, P. Gao, X. Wang and W. Hu, *Chem. Soc. Rev.*, 2023, **52**, 1650–1671.
117 S. Lahiri, D. Mandal, S. Biswas, P. R. Gogate and R. L. Bhardwaj, *Ultrason. Sonochem.*, 2022, **82**, 105863.
118 S. Aldroubi, E. Anglaret, I. B. Malham, P. Hesemann, N. Brun and A. Mehdi, *J. Colloid Interface Sci.*, 2023, **636**, 668–676.
119 J. Tang, Q. Wang, J. Tian, X. Li, N. Li, Y. Peng, X. Li, Y. Zhao, C. He, S. Wu, J. Li, Y. Guo, B. Huang, Y. Chu, Y. Ji, D. Shang, L. Du, R. Yang, W. Yang, X. Bai, D. Shi and G. Zhang, *Nat. Commun.*, 2023, **14**, 3633.
120 X. Liu, P. Ding, H. Li, Z. Yuan, Y. Jiao and S. Jameh-Bozorghi, *Microporous Mesoporous Mater.*, 2020, **299**, 110127.
121 Y. Du, Y. Zhang, R. Zhang and S. Lin, *ACS Appl. Nano Mater.*, 2021, **4**, 11088–11096.
122 H. Lee, M. Koo, C. Park, M. Patel, H. Han, T. H. Park, P. Kumar, W. Koh and C. Park, *Nano Res.*, 2020, **13**, 2726–2734.
123 R. Mehta, M. Min, R. F. Hossain, G. A. Saenz, G. Gamboa and A. B. Kaul, *Nano Res.*, 2023, **16**, 7858–7866.
124 C. Xu, P. He, J. Liu, A. Cui, H. Dong, Y. Zhen, W. Chen and W. Hu, *Angew. Chem., Int. Ed.*, 2016, **55**, 9519–9523.
125 F. Arjmand, H. Aghaie, M. Bahadori and K. Zare, *J. Mol. Liq.*, 2019, **277**, 80–83.
126 H. Esmaeili and H. Hashemipour, *J. Mol. Liq.*, 2021, **324**, 114660.
127 N. Pellens, N. Doppelhammer, S. Radhakrishnan, K. Asselman, C. V. Chandran, D. Vandenabeele, B. Jakoby, J. A. Martens, F. Taulelle, E. K. Reichel, E. Breynaert and C. E. A. Kirschhock, *Chem. Mater.*, 2022, **34**, 7139–7149.
128 F. Liu, A. Li, J. Wang and Z. Luo, *Energy*, 2021, **214**, 119034.
129 J. Shen, Y. He, C. Gao, B. Yang, X. Tao, M. Wang and G. Ye, *Colloids Surf., A*, 2022, **653**, 130025.
130 J. Shen, Y. He, C. Gao, X. Tao, B. Yang, M. Wang and G. Ye, *ACS Appl. Mater. Interfaces*, 2023, **15**, 13724–13729.
131 R. Chang, Q. Chen, W. Shen, Y. Zhang, B. Zhang and S. Wang, *Adv. Funct. Mater.*, 2023, **33**, 2301010.
132 D. Vaquero, V. Clericò, J. Salvador-Sánchez, J. Quereda, E. Diez and A. M. Pérez-Muñoz, *Micromachines*, 2021, **12**, 1576.
133 S. Z. Bisri, S. Shimizu, M. Nakano and Y. Iwasa, *Adv. Mater.*, 2017, **29**, 1607054.
134 T. Itani, P. P. Naulleau, E. Hendrickx, P. A. Gargini, K. G. Ronse, A. Ko, S. Thibaut, E. Liu, C. A. Mack and A. Raley, presented in part at the International Conference on Extreme Ultraviolet Lithography 2018, 2018.
135 D. F. Sunday, X. Chen, T. R. Albrecht, D. Nowak, P. Rincon Delgadillo, T. Dazai, K. Miyagi, T. Maehashi, A. Yamazaki, P. F. Nealey and R. J. Kline, *Chem. Mater.*, 2020, **32**, 2399–2407.
136 S. Chen, G. Wu, X. Wang, X. Chen and P. Nealey, *ACS Appl. Polym. Mater.*, 2019, **2**, 427–436.
137 H. Hao, S. Chen, J. Ren, X. Chen and P. Nealey, *Nanotechnology*, 2023, **34**, 205303.
138 L. Liu, K. Song, T. Feng, T. Song, J. Li, S. Chen, W. Zhao and S. Zhang, *Green Chem.*, 2023, **25**, 5989–5998.
139 Z. Zhang, S. Ding, D. Xia and J. Xu, *ACS Macro Lett.*, 2023, **12**, 1005–1011.
140 K. Rola, A. Zajac, M. Czajkowski, M. Fiedot-Tobola, A. Szpecht, J. Cybinska, M. Smiglak and K. Komorowska, *Langmuir*, 2019, **35**, 11968–11978.
141 K. P. Rola, A. Zając, A. Szpecht, D. Kowal, J. Cybińska, M. Śmiglak and K. Komorowska, *Eur. Polym. J.*, 2021, **156**, 110615.
142 G. Zhang, Y. Guo, Y. Fang, Y. Chu and Z. Liu, *J. Mater. Chem. C*, 2023, **11**, 5882–5889.
143 F. Pena-Pereira, A. Kloskowski and J. Namieśnik, *Green Chem.*, 2015, **17**, 3687–3705.
144 Z. Li, Q. Han, K. Wang, S. Song, Y. Xue, X. Ji, J. Zhai, Y. Huang and S. Zhang, *Catal. Rev.*, 2022, 484–530.
145 Q. Han, Y. Su, K. M. Smith, J. Binns, C. J. Drummond, C. Darmanin and T. L. Greaves, *J. Colloid Interface Sci.*, 2023, **650**, 1393–1405.
146 A. A. Elgharbawy, M. Moniruzzaman and M. Goto, *Biochem. Eng. J.*, 2020, **154**, 107426.
147 A. A. M. Elgharbawy, M. Moniruzzaman and M. Goto, *Curr. Opin. Green Sustainable Chem.*, 2021, **27**, 100406.
148 C. Molina-Fernández, A. Péters, D. P. Debecker and P. Luis, *Biochem. Eng. J.*, 2022, **187**, 108639.
149 J. M. Gomes, S. S. Silva and R. L. Reis, *Chem. Soc. Rev.*, 2019, **48**, 4317–4335.
150 R. Villa, E. Alvarez, R. Porcar, E. Garcia-Verdugo, S. V. Luis and P. Lozano, *Green Chem.*, 2019, **21**, 6527–6544.
151 P. Wolski, B. W. Blankenship, A. Umar, M. Cabrera, B. A. Simmons, K. L. Sale and E. C. Achinivu, *Front. Energy Res.*, 2023, **11**, DOI: **10.3389/fenrg.2023.1212719**.
152 R. Wakayama, S. Uchiyama and D. Hall, *Biophys. Rev.*, 2019, **11**, 209–225.
153 A. A. M. Elgharbawy, M. Moniruzzaman and M. Goto, *Biochem. Eng. J.*, 2020, **154**, 107426.
154 J. Dupont, B. C. Leal, P. Lozano, A. L. Monteiro, P. Migowski and J. D. Scholten, *Chem. Rev.*, 2024, **124**, 5227–5420.
155 M. Sivapragasam, M. Moniruzzaman and M. Goto, *Biotechnol. J.*, 2016, **11**, 1000–1013.
156 J. M. Costa, T. Forster-Carneiro and J. P. Hallett, *Green Chem.*, 2024, **26**, 705–719.
157 Y. Zhuo, H. L. Cheng, Y. G. Zhao and H. R. Cui, *Pharmaceutics*, 2024, **16**, 151.
158 R. Md Moshikur and M. Goto, *Chem. Rec.*, 2023, **23**, e202300026.
159 X. Ji, Y. Xue, Z. Li, Y. Liu, L. Liu, P. K. Busk, L. Lange, Y. Huang and S. Zhang, *Green Chem.*, 2021, **23**, 6990–7000.
160 X. Ji, H. Guo, Y. Xue, Y. Huang and S. Zhang, *Renewable Sustainable Energy Rev.*, 2023, **188**, 113809.
161 X. Qiu, Y. Wang, Y. Xue, W. Li and Y. Hu, *Chem. Eng. J.*, 2020, **391**, 123564.

162 S. Malla, K. J. Jisha, R. L. Gardas and S. N. Gummadi, *J. Mol. Liq.*, 2021, **328**, 115394.
163 Q. Wang, L. Sheng, X. Guo, R. Chen, C. Zhou and F. Yang, *Appl. Catal., A*, 2023, **666**, 119426.
164 H. Suo, M. Li, R. Liu and L. Xu, *Colloids Surf., B*, 2021, **206**, 111960.
165 L. Peng, Z. Wang, H. Zhu, T. Zeng, W. Zhou, S. Yao and H. Song, *J. Mol. Liq.*, 2021, **342**, 116938.
166 Z. Zhou, X. Ju, M. Zhou, X. Xu, J. Fu and L. Li, *Bioresour. Technol.*, 2019, **294**, 31536857.
167 M. Zhou, L. Yan, H. Chen, X. Ju, Z. Zhou and L. Li, *Fuel*, 2021, **304**, 121484.
168 A. Escudero, A. P. de Los Rios, C. Godinez, F. Tomas and F. J. Hernandez-Fernandez, *Molecules*, 2020, **25**, 3233.
169 S. M. Ghorbani, M. R. Housaindokht and M. R. Bozorgmehr, *J. Mol. Liq.*, 2021, **332**, 115850.
170 S. Ghanbari-Ardestani, S. Khojasteh-Band, M. Zaboli, Z. Hassani, M. Mortezavi, M. Mahani and M. Torkzadeh-Mahani, *J. Mol. Liq.*, 2019, **292**, 111318.
171 X. Zhang, Y. Xue, Z. Lu, H. Xu and Y. Hu, *Bioprocess Biosyst. Eng.*, 2022, **45**, 749–759.
172 X. Ji, Y. Xue, Z. Li, Y. Liu, L. Liu, P. K. Busk, L. Lange, Y. Huang and S. Zhang, *Green Chem.*, 2021, **23**, 6990–7000.
173 K. Liu, S. Wang, L. Duan, L. Jiang and S. Wang, *Biochem. Eng. J.*, 2021, **176**, 108175.
174 M. Wu, J. Hu, Y. Wu, Y. Tang, Y. Zhang, Y. Guan, Z. Lou, Z. Yu and J. Yu, *Chemosphere*, 2021, **281**, 130913.
175 Z. Li, K. Wang, Y. Xue, K. Lin, X. Ji and Y. Huang, *ACS Sustainable Chem. Eng.*, 2023, **11**, 4197–4208.
176 A. A. M. Elgharbawy, M. Moniruzzaman and M. Goto, *Curr. Opin. Green Sustainable Chem.*, 2021, **27**, 100406.
177 K. C. Badgujar, V. C. Badgujar and B. M. Bhanage, *Curr. Opin. Green Sustainable Chem.*, 2022, **36**, 100621.
178 A. Schindl, M. L. Hagen, S. Muzammal, H. A. D. Gunasekera and A. K. Croft, *Front. Chem.*, 2019, **7**, 347.
179 Q. Wang, M. Ge, X. Guo, Z. Li, A. Huang, F. Yang and R. Guo, *Appl. Catal., A*, 2021, **626**, 118350.
180 S. Prots, M. L. C. Passos, R. A. S. Lapa and M. L. M. F. S. Saraiva, *Process Biochem.*, 2021, **108**, 121–128.
181 M. Moniruzzaman, N. Kamiya, K. Nakashima and M. Goto, *Green Chem.*, 2008, **10**, 497–500.
182 I. V. Pavlidis, D. Gournis, G. K. Papadopoulos and H. Stamatis, *J. Mol. Catal. B: Enzym.*, 2009, **60**, 50–56.
183 J. K. Lee and M. J. Kim, *J. Org. Chem.*, 2002, **67**, 6845–6847.
184 P. Hara, U. Hanefeld and L. T. Kanerv, *Green Chem.*, 2009, **11**, 250–256.
185 T. Itoh, Y. Matsushita, Y. Abe, S. H. Han, S. Wada, S. Hayase, M. Kawatsura, S. Takai, M. Morimoto and Y. Hirose, *Chem. – Eur. J.*, 2006, **12**, 9228–9237.
186 T. Itoh, S. Han, Y. Matsushita and S. Hayase, *Green Chem.*, 2005, **7**, 621–621.
187 H. Fernandez Fj, *J. Bioprocess. Biotech.*, 2018, **8**, 1–2.
188 H. Suo, L. Xu, Y. Xue, X. Qiu, H. Huang and Y. Hu, *Carbohydr. Polym.*, 2020, **234**, 115914.
189 N. Chen, C. Zhang, X. Dong, Y. Liu and Y. Sun, *Biochem. Eng. J.*, 2020, **158**, 107557.
190 W. Zhang, Y. Zhang, Z. Lu, B. Nian, S. Yang and Y. Hu, *J. Environ. Manage.*, 2023, **346**, 118975.
191 J. C. Stevens, D. W. Rodgers, C. Dumon and J. Shi, *Front. Energy Res.*, 2020, **8**, 158.
192 J. L. Shamshina and R. D. Rogers, *Chem. Rev.*, 2023, **123**, 11894–11953.
193 G. Iyer, S. Dyawanapelly, R. Jain and P. Dandekar, *Int. J. Biol. Macromol.*, 2022, **208**, 565–585.
194 C. M. Hamadani, I. Chandrasiri, M. L. Yaddehige, G. S. Dasanayake, I. Owolabi, A. Flynt, M. Hossain, L. Liberman, T. P. Lodge, T. A. Werfel, D. L. Watkins and E. E. L. Tanner, *Nanoscale*, 2022, **14**, 6021–6036.
195 A. M. Curreri, S. Mitragotri and E. E. L. Tanner, *Adv. Sci.*, 2021, **8**, e2004819.
196 J. Yuan, N. Zhou, J. Wu, T. Yin and Y. Jia, *RSC Adv.*, 2022, **12**, 3416–3422.
197 Y. Gao, W. Zhang, Y. Wei, Y. Li, T. Fei, Y. Shu and J. Wang, *Biomater. Sci.*, 2022, **10**, 1041–1052.
198 Y. Shi, Z. Zhao, Y. Gao, D. Pan, A. K. Salinas, E. E. L. Tanner, J. Guo and S. Mitragotri, *J. Controlled Release*, 2020, **322**, 602–609.
199 B. Lu, G. Zhou, F. Xiao, Q. He and J. Zhang, *J. Mater. Chem. B*, 2020, **8**, 7994–8001.
200 K. Niesyto, A. Mazur and D. Neugebauer, *Materials*, 2022, **15**, 4457.
201 H. Albadawi, Z. Zhang, I. Altun, J. Hu, L. Jamal, K. N. Ibsen, E. E. L. Tanner, S. Mitragotri and R. Oklu, *Sci. Transl. Med.*, 2021, **13**, eabe3889.
202 W. Tang, B. Liu, S. Wang, T. Liu, C. Fu, X. Ren, L. Tan, W. Duan and X. Meng, *RSC Adv.*, 2016, **6**, 32434–32440.
203 Y. Yu, Q. Wu, M. Niu, L. Gou, L. Tan, C. Fu, X. Ren, J. Ren, Y. Zheng and X. Meng, *Biomater. Sci.*, 2022, **10**, 3503–3513.
204 S. Rasouli, S. Davaran, F. Rasouli, M. Mahkam and R. Salehi, *Des. Monomers Polym.*, 2013, **17**, 227–237.
205 B. Lu, S. Hu, D. Wu, C. Wu, Z. Zhu, L. Hu and J. Zhang, *J. Mater. Chem. B*, 2022, **10**, 1226–1235.
206 R. Md Moshikur, M. R. Chowdhury, M. Moniruzzaman and M. Goto, *Green Chem.*, 2020, **22**, 8116–8139.
207 A. R. Jesus, L. R. Raposo, M. R. C. Soromenho, D. A. S. Agostinho, J. M. S. S. Esperança, P. V. Baptista, A. R. Fernandes and P. M. Reis, *Symmetry*, 2021, **13**, 2053.
208 Z. Sidat, T. Marimuthu, P. Kumar, L. C. du Toit, P. P. D. Kondiah, Y. E. Choonara and V. Pillay, *Pharmaceutics*, 2019, **11**, 96.
209 B. Yang, Y. Chen and J. Shi, *Adv. Mater.*, 2019, **31**, 1901778.
210 Y. Zhu and F. Chen, *Chem. Rev.*, 2014, **114**, 6462–6555.
211 R. Zha, R. Wu, Y. Zong, Z. Wang, T. Wu, Y. Zhong, H. Liang, L. Chen, C. Li and Y. Wang, *Talanta*, 2023, **258**, 124377.
212 C. Liu, Q. Deng, G. Fang, M. Dang and S. Wang, *Anal. Biochem.*, 2017, **530**, 50–56.
213 M. M. Pereira, J. D. Calixto, A. C. A. Sousa, B. J. Pereira, Á. S. Lima, J. A. P. Coutinho and M. G. Freire, *Sci. Rep.*, 2020, **10**, 14931.

214 X. Ding, C. Liu, W. Yu and Z. Liu, *Talanta*, 2023, **262**, 124690.
215 J. Liu, J. Wang, T. Wang, D. Li, F. Xi, J. Wang and E. Wang, *Biosens. Bioelectron.*, 2015, **65**, 281–286.
216 D. Yadav and P. Kumar, *Neurochem. Int.*, 2022, **156**, 105327.
217 B. Iqbal, N. Muhammad, A. Jamal, P. Ahmad, Z. U. H. Khan, A. Rahim, A. S. Khan, G. Gonfa, J. Iqbal and I. U. Rehman, *J. Mol. Liq.*, 2017, **243**, 720–725.
218 Y. Yu, Z. Yang, S. Ren, Y. Gao and L. Zheng, *J. Mol. Liq.*, 2020, **299**, 112185.
219 A. N. Duman, I. Ozturk, A. Tuncel, K. Ocakoglu, S. G. Colak, M. Hosgor-Limoncu and F. Yurt, *Heliyon*, 2019, **5**, e02607.
220 P. Bonyadi and K. Amini, *Folia Microbiol.*, 2022, **67**, 777–784.
221 X. Zhang, J. Zheng, P. Jin, D. Xu, S. Yuan, R. Zhao, S. Depuydt, Y. Gao, Z. Xu and B. Van der Bruggen, *J. Hazard. Mater.*, 2022, **435**, 129010.
222 J. Shi, M. Wang, Z. Sun, Y. Liu, J. Guo, H. Mao and F. Yan, *Acta Biomater.*, 2019, **97**, 247–259.
223 I. Ali, A. Haque, K. Saleem and M. F. Hsieh, *Bioorg. Med. Chem.*, 2013, **21**, 3808–3820.
224 O. A. Abu Ali, W. Abd El-Fattah, M. Y. Alfaifi, A. A. Shati, S. E. I. Elbehairi, A. H. Abu Almaaty, R. F. M. Elshaarawy and E. Fayad, *Inorg. Chim. Acta*, 2023, **551**, 121460.
225 Sangeeta, Sonaxi, R. Tomar, S. Agrawal and A. Sarkar, *ChemistrySelect*, 2023, **8**, e202204535.